INSTITUTO NACIONAL DE PESQUISAS DA AMAZÔNIA – INPA
UNIVERSIDADE DO ESTADO DO AMAZONAS – UEA
Programa de Pós-Graduação em Clima e Ambiente – PPG-CLIAMB

UM PROBLEMA DE INTERAÇÃO OCEANO-ATMOSFERA-BIOSFERA: ALTERAÇÕES POTENCIAIS NA VEGETAÇÃO DA AMÉRICA DO SUL DEVIDAS AO AQUECIMENTO GLOBAL

MARCOS PAULO SANTOS PEREIRA

Manaus, Amazonas
Outubro, 2011.

MARCOS PAULO SANTOS PEREIRA

UM PROBLEMA DE INTERAÇÃO OCEANO-ATMOSFERA-BIOSFERA: ALTERAÇÕES POTENCIAIS NA VEGETAÇÃO DA AMÉRICA DO SUL DEVIDO AO AQUECIMENTO GLOBAL

Orientador: Dr. Marcos Heil Costa

Tese apresentada ao Instituto Nacional de Pesquisa da Amazônia e Universidade do Estado do Amazonas como parte dos requisitos para obtenção do título de Doutor em Clima e Ambiente, área de concentração: Geociências.

Manaus, Amazonas

Outubro, 2011.

Ficha Catalográfica

P436 Pereira, Marcos Paulo Santos
Um problema de interação oceano-atmosfera-biosfera: alterações potenciais na vegetação da América do Sul devidas ao aquecimento global / Marcos Paulo Santos Pereira. --- Manaus : [s.n.], 2011.
x, 65 f. : il. (algumas color.)

Tese (Clima e Ambiente)--INPA/UEA, Manaus, 2011.
Orientador: Dr. Marcos Heil Costa
Área de concentração: Interações Clima-Biosfera na Amazônia

1.Dinâmica da vegetação – América do Sul 2.Mudanças climáticas 3.Interação oceano-atmosfera-biosfera I.Título

CDD 19ª ed. 551.6

Dados Internacionais de Catalogação na Publicação (CIP)

Sinopse:

Estudou-se a mudanças na estrutura da vegetação na América do Sul em função de diferentes cenários de clima para a primeira metade do século XXI, em particular considerando diferentes padrões de temperatura da superfície do mar.

Palavras-chave: Vegetação dinâmica, mudanças climáticas, incertezas das projeções climáticas.

Dedico

Aos meus pais João José Pereira (in memorian) e Maria Terezinha dos Santos, e ao meu tio José dos Santos (in memorian).

Agradecimentos

Neste trabalho não poderia deixar de expressar o meu sincero agradecimento às pessoas que cooperaram para a concretização desta pesquisa. Assim, as minhas palavras de gratidão vão para:

- a Deus que me deu o dom da vida e entre outras coisas a possibilidade de realizar meus objetivos.
- à minha família, em especial a minha mãe. Mesmo estando longe, vocês nunca deixaram de me incentivar e de acreditar em mim. Obrigado a todos vocês por tudo!
- à Universidade do Estado do Amazonas (UEA) e ao Instituto de Pesquisas da Amazônia (INPA), pela oportunidade de participar de seu programa de pós-graduação e utilização de suas instalações.
- à Fundação de Amparo a Pesquisa do Estado do Amazonas (FAPEAM), pela concessão de bolsa de estudo.
- ao meu orientador, Professor Marcos Heil Costa, pela oportunidade concedida, dedicação, disponibilidade, sugestões, ensinamentos, amizade e colaboração em todas as fases de desenvolvimento deste trabalho.
- à Ana Cláudia Mendes Malhado, pelo apoio, atenção, disponibilidade, contribuições e sugestões dadas no desenvolvimento deste trabalho.
- ao Flavio Justino, pela atenção, sugestões e contribuições em algumas fases deste trabalho.
- aos professores do curso de Clima e Ambiente, pelo conhecimento que me foram passados durante esses anos em que estivemos juntos.
- aos amigos do grupo de pesquisa em Interação Atmosfera-Biosfera pela amizade formada no grupo de pesquisa e esclarecimento de dúvidas ao longo deste trabalho, estão deixando mais uma vez saudades.
- aos amigos da Terra Du Nunca, os últimos anos não teriam sido divertidos sem a ajuda e companhia dos Brothers.
- aos amigos de Manaus e do programa Cliamb, pelos momentos de descontração e carinho.

Resumo

Uma das consequências esperadas para o aquecimento global é mudanças na distribuição e estrutura da vegetação. Poucos estudos avaliaram o comportamento dinâmico da vegetação tropical num cenário de CO_2 elevado, e estes poucos encontraram resultados contraditórios para a vegetação da América do Sul. Uma das possíveis explicações para esses resultados conflitantes são os diferentes padrões de temperatura da superfície do mar (TSM) usados nas simulações. Esta tese examina as mudanças na estrutura da vegetação na América do Sul em função de diferentes cenários de clima para a primeira metade do século XXI, em particular considerando diferentes padrões de TSM. Neste estudo foram realizados experimentos climáticos usando um modelo acoplado de clima-vegetação para o cenário A2 do IPCC, com dez diferentes padrões de TSM. Inicialmente, observa-se que as diferentes previsões para a TSM para a primeira metade do século XXI aumentam a incerteza associada com as previsões futuras da distribuição dos principais ecossistemas da América do Sul. A incerteza na capacidade de prever os padrões de vegetação futuro aumenta de tal forma que a simulação até 2050 não é capaz de prever com robustez a cobertura vegetal de uma área equivalente a 28% da América do Sul (5×10^6 km²). Os resultados mostram que a variabilidade espaço-temporal da TSM exerce uma forte influência sobre a dinâmica da vegetação, havendo uma considerável variação na direção e magnitude dos efeitos da TSM em diferentes regiões na América do Sul. Além disso, as simulações mostram que certos padrões de TSM para 2011-2050 podem ocasionar a diminuição das áreas de floresta tropical e savana, e que essas áreas serão ocupadas principalmente por floresta decídua. Assim, o uso de diferentes padrões de TSM nos modelos acoplados clima-vegetação é extremamente importante para melhores projeções futuras da cobertura vegetal.

Abstract

One of the expected consequences of global warming is change in the distribution and structure of vegetation. Few studies have evaluated the dynamic behavior of tropical vegetation against a backdrop of elevated CO_2, with mixed results for the vegetation in South America. One possibility to explain the opposite results are different patterns of sea surface temperature (SST) used in the simulations. This thesis determines the changes in vegetation structure in South America caused by different climate scenarios for the first half of the 21th century, especially considering the different patterns of SST. In this study were climate experiments using a coupled climate-vegetation model for the A2 IPCC scenario, with ten different patterns of the SST. Initially, it is demonstrated how different predictions for SST for the first half of 21th century increase the uncertainty associated with forecasts of the future distribution of major ecosystems in South America. The increasing uncertainty in the ability to forecast future vegetation patterns is such that by 2050 it is unable to robustly forecast the vegetation cover in an area equivalent to 28% in South America (5×10^6 km²). The results show that the spatial-temporal variability in SST exerts a strong influence over the vegetation dynamics, there considerable variation in the direction and magnitude of SST effects in different South American regions. However, the simulations for 2011-2050 show that certain patterns of SST are likely to decrease the tropical evergreen rainforest and savanna, and that these areas will be occupied mainly by tropical seasonal rainforest. Thus, the use of different SST patterns in coupled climate-vegetation models is clearly important for improving projections of future vegetation cover in this region.

Sumário

Lista de Figuras

Capítulo 1: Vegetation patterns in South America associated with rising CO_2: uncertainties related to sea surface temperatures.

Capítulo 2: Response of South American terrestrial ecosystem to future patterns of Sea Surface Temperature

Introdução Geral

Atualmente, uma das preocupações mais críticas da humanidade refere-se às mudanças climáticas futuras. O Painel Intergovernamental sobre Mudança do Clima (IPCC, 2007) estima que a temperatura média da superfície global aumentou 0,74°C ± 0,18°C, nos últimos 100 anos (1906-2005). A taxa de aquecimento nos últimos 50 anos foi quase o dobro da taxa observada nos últimos 100 anos (0,13°C ± 0,03°C contra 0,07 ± 0,02°C por década) (Trenberth et al., 2007). A maior parte do aumento observado nas temperaturas médias globais desde meados do século XX se deve, provavelmente, ao aumento nas concentrações de gases do efeito estufa antropogênico (Hegerl et al., 2007). O maior aumento na queima de combustíveis fósseis aconteceu nas últimas décadas, e dez dos dez anos mais quentes já registrados ocorreram depois de 1990 (Mokhov et al., 2002). De todas as partes do mundo, governos e comunidades de cientistas expressam preocupações e dedicam atenção a este fenômeno, o aquecimento global, que pode ter como consequências: fortes ondas de calor; intensificação do volume e frequência das precipitações em algumas partes do globo e secas em outras; intensificações dos ciclones tropicais, tufões e furacões; aumento do nível do mar; alterações na produtividade das culturas; e até mesmo as florestas mais remotas e aparentemente intocadas podem ser afetadas pelo aquecimento global.

A vegetação é o espelho do clima, com o qual interage de maneira bidirecional (Foley et al., 2000). Assim, é esperado que mudanças no clima afetem a distribuição e estrutura da vegetação, que por sua vez retroalimentam a circulação atmosférica, provocando alterações climáticas adicionais.

Além do efeito radiativo das moléculas de CO_2 na atmosfera (efeito estufa), alguns estudos verificaram a existência de dois outros efeitos do CO_2 sobre a vegetação e o clima: o acréscimo da concentração de CO_2 atmosférico pode estimular a fotossíntese líquida, aumentar a eficiência do uso da água na maioria das plantas (Polley et al., 1993; Field et al., 1995; Curtis, 1996; Sellers et al., 1997) – chamada de efeito fisiológico do CO_2 – e modificar a composição e estrutura dos ecossistemas – chamado de efeito estrutural, ou ecológico do CO_2 (Betts et al., 1997). Até o momento, os cenários do IPCC consideraram uma vegetação fixa, isto é, não avaliaram nem os efeitos fisiológicos nem os estruturais da elevação do CO_2 e da mudança climática na vegetação, nem as retroalimentações decorrentes.

Mesmo se tratando de estudos de alta relevância, até o momento poucos experimentos avaliaram o comportamento dinâmico da vegetação tropical num cenário de CO_2 elevado, considerando tanto os efeitos radiativos, como os fisiológicos e ecológicos. No primeiro desses estudos, Levis et al. (2000) usaram o modelo climático NCAR GENESIS 2.0 acoplado ao modelo de dinâmica de vegetação IBIS 2.0. Para a região tropical, suas simulações demonstraram que o aumento de CO_2 foi acompanhado de aumento na cobertura vegetal, dando início a uma retroalimentação através do ciclo hidrológico, que levou a um acréscimo na precipitação e da umidade dos solos. Por outro lado, os estudos de Cox et al. (2000, 2004) e Betts et al. (2004) examinaram os efeitos de um cenário de CO_2 elevado no sistema climático, usando o modelo HadCM3, e encontraram forte redução na precipitação sobre a Amazônia, aparentemente devido aos efeitos radiativos do aumento do CO_2, provocando a morte da floresta Amazônica e como consequência uma diminuição ainda maior da precipitação.

Uma das possibilidades para explicar os resultados opostos de Levis et al. (2000) e Cox et al. (2000) são os diferentes padrões de temperatura da superfície do mar (TSM) usados nas duas simulações, uma vez que o clima da América do Sul é fortemente dependente dos padrões de TSM do Pacífico e do Atlântico (Nobre e Shukla, 1996; Diaz et al., 1998; Grimm et al., 2000; Haylock et al., 2006). De acordo com Fu et al. (2001), a sazonalidade da TSM no Pacífico e Atlântico Tropicais tem grande influência na precipitação no Leste da Amazônia durante os equinócios, que são controladas pela zona de convergência intertropical (ITCZ) e por ondas de Rossby. Esses processos são amplificados pelos ciclos sazonais da TSM. A TSM afeta bem menos a precipitação Amazônica durante os solstícios e tem pouca influência na região Oeste da Amazônia. Outra evidência dos impactos da TSM no clima regional também pode ser vista durante os eventos de El Niño – Oscilação Sul (ENSO) (Grimm et al., 2000), Oscilação Decadal do Pacífico (PDO) (Andreoli e Kayano, 2005) e Oscilação Multidecadal do Atlântico (AMO), que tem sido associada com a variabilidade das anomalias climáticas na América do Sul.

A geração atual de modelos climáticos acoplados oceano-atmosfera apresenta diferentes padrões da TSM para os trópicos, mesmo quando executados para um mesmo cenário de CO_2 (Barsugli et al., 2006). A ligação entre a TSM e o clima regional tem potencial para aumentar dramaticamente a incerteza das previsões de cobertura da vegetação. Incertezas nas projeções dos modelos climáticos são muitas vezes caracterizados por conhecimento incompleto dos fatores externos que influenciam o sistema climático (forçantes – cenários incertos), diferentes codificações nas formulações numéricas e físicas dos modelos

(diferentes respostas dos modelos), e variabilidade natural do sistema climático (variabilidade interna do modelo) (Hawkins e Sutton, 2009; Tebaldi e Knutti, 2007). Caracterização e quantificação da incerteza nas projeções de mudanças climáticas são de fundamental importância não só para fins de detecção e atribuição, mas também por razões estratégicas para adaptação e mitigação.

Tais mudanças climáticas terão efeitos em cadeia sobre a vegetação. Por exemplo, quando Jiang et al. (2011) forçaram um modelo acoplado clima-vegetação por padrões de gelo oceânico e TSM futuro (projetado com 17 modelos de circulação geral de oceano-atmosfera que participam do quarto relatório de avaliação do IPCC, e pelas concentrações atmosférica do CO_2 no cenário de emissões A2), a vegetação é prevista para se tornar mais densa (em termos do aumento da média global do índice da área foliar). Embora os estudos citados acima já investigaram os efeitos de retroalimentação da vegetação sobre aquecimento global, eles não levam em consideração o comportamento da vegetação em relação à variabilidade da TSM ou estão limitados a determinadas regiões da América do Sul, e que deve ser estudado mais profundamente, devido tanto à sua importância científica quanto às suas potenciais aplicações para a sociedade.

Objetivos

Considerando o exposto, o objetivo geral desta tese é determinar mudanças na estrutura da vegetação na América do Sul em função de diferentes cenários de clima para a primeira metade do século XXI, em particular considerando diferentes padrões de temperatura da superfície do mar.

Para isso, é preciso atingir os seguintes objetivos específicos:

- Validar o modelo climático, utilizando banco de dados históricos.
- Quantificar a incerteza nas previsões da vegetação para América do Sul causada por diferentes padrões de TSM.
- Avaliar a influência da variabilidade espaço-temporal da TSM sobre a dinâmica da vegetação na América do Sul, em cenário de aquecimento global.
- Investigar os impactos da TSM sobre a vegetação na Amazônia.

Hipótese a ser testada: Diferentes padrões de TSM do Pacífico e do Atlântico têm papel fundamental na definição da cobertura vegetal na América do Sul, em cenários de aquecimento global.

Além desta Introdução Geral, esta tese tem três capítulos principais (que são apresentados no formato de artigo cientifico, e um capitulo de Conclusão (Síntese). O primeiro capítulo demonstra como as diferentes previsões de TSM para a primeira metade do século XXI aumentam a incerteza associada com as previsões da distribuição futura dos maiores ecossistema na América do Sul. O segundo capítulo investiga como a vegetação na América do Sul responde aos padrões futuros da TSM do Pacifico e Atlântico, sob aquecimento global e cenário de não aquecimento. O terceiro capítulo produz previsões para a cobertura vegetal na região da Amazônia, sob condições de aquecimento global e os relaciona a diferentes padrões de TSM. Finalmente, a Conclusão discute os principais resultados de todos os capítulos e apresenta sugestões para pesquisas futuras.

Capítulo 1

Pereira, M.P.S. and Costa, M.H. **Vegetation patterns in South America associated with rising CO_2: uncertainties related to sea surface temperatures.** Submitted manuscript to Climatic Change, in review.

Abstract Spatially precise forecasts of the impacts of climate change on the distribution of major vegetation types are essential for the implementation of effective conservation and land use policy. However, existing studies frequently omit major sources of climate variability that can significantly increase the uncertainty of projections. In this study we demonstrate how different predictions for sea surface temperature (SST) for the first half of 21th century increase the uncertainty associated with forecasts of the future distribution of major ecosystems in South America. This is demonstrated through a numerical experiment using a coupled climate-vegetation model (CCM3-IBIS) for IPCC emission scenario A2 that incorporates the SST data from ten different models. The study reveals an increasing uncertainty in the ability to forecast future vegetation patterns, such that by 2050 the simulation is unable to robustly forecast the vegetation cover in an area equivalent to 28% in South America (5×10^6 km²). The future of the central and northeastern regions of Brazil is especially uncertain, with outcomes, ranging from savanna, and open shrubland to grassland. Recognizing and managing such uncertainty should be a priority for decision makers.

Keywords: Vegetation dynamics; Climate change; climate models; ocean-atmosphere-biosphere interaction;

1 Introduction

Patterns of natural vegetation are determined by a combination of temperature, rainfall, solar radiation, soil conditions and CO_2 concentration (Woodward and Kelly 2004). Thus, changes in climate due to rising CO_2 will affect the distribution and structure of vegetation, which in

turn feedback on atmospheric circulation, causing further climate change. In addition to rising temperatures CO_2 may have at least two additional effects on vegetation: (1) A physiological effect whereby the increase in atmospheric CO_2 concentration stimulates net photosynthesis, thereby increasing water use efficiency of most plants (Field et al. 1995; Sellers et al. 1996); (2) A structural effect whereby changes in plant physiology alters the composition and structure of ecosystems (Betts et al. 1997).

Despite the dynamic nature of vegetation-climate interactions, the standard scenarios of Intergovernmental Panel on Climate Change (IPCC) consider vegetation to be "fixed", in the sense that neither the structural nor physiological effects are evaluated. However, incorporating such information into global climate models is not straightforward. Studies on the response of tropical vegetation elevated CO_2 have produced conflicting results. For example, Levis et al. (2000) simulated the interactions between radiative forcing, physiological effects, and vegetation cover at a global level using the NCAR GENESIS 2.0 climate model coupled to the vegetation dynamics model IBIS 2.0. For the tropical region, the simulations indicated that an increase in CO_2 is accompanied by an increase in vegetation cover. This process initiated a feedback loop through the hydrological cycle, leading to an increase in precipitation and soil moisture. In contrast, studies by Cox et al. (2000, 2004) and Betts et al. (2004) using the HadCM3 model suggest that the Amazon region will suffer a significant decline in rainfall leading to the rapid loss of rainforest and, as a consequence, a further decrease in rainfall.

The contrasting results may be due to different patterns of sea surface temperature (SST) used by the simulations since the South American climate is strongly dependent on the patterns of SST in the Pacific and Atlantic (Nobre and Shukla 1996; Diaz et al. 1998; Grimm et al. 2000; Haylock et al. 2006). According to Fu et al. (2001), the seasonality of SST in the Tropical Pacific and Atlantic has a major influence on precipitation in eastern Amazonia during equinoxes. The eastern part of Amazonia is thought to be influenced by the direct thermal circulation of the Intertropical Convergence Zone (ITCZ) and Rossby waves - these processes being amplified by seasonal cycles of SST. Moreover, SST has less effect on the precipitation during the solstices and has little influence in western Amazonia. Further evidence of SST impacts on regional climate can also be seen during El Niño and La Niña events which have been associated with a range of climate anomalies in South America (Grimm et al. 2000). The current generation of coupled ocean-atmosphere climate models generates a range of patterns of SST for the tropics, even when performed for the same future

scenario of CO_2 (Barsugli et al. 2006). This link between SST and regional climate therefore has the potential to dramatically increase the uncertainty of vegetation cover forecasts.

The objective of this study is to quantify the uncertainty in vegetation forecasts for South America caused by different predicted patterns of SST for the first half of the 21th century. We hypothesize that under the same greenhouse gas emissions scenario, varying patterns of Pacific and Atlantic SST will play a major role in defining the spatial distribution and identity of vegetation cover in South America.

2 Model description and experiment design

Simulations were performed using the CCM3 (Community Climate Model) general circulation model (Kiehl et al. 1998) coupled to the surface model IBIS (Integrated Biosphere Simulator) - a dynamic global vegetation model which considers changes in the composition and structure of vegetation in response to environmental conditions (detailed description in Delire et al. 2002). The simulations were performed at T42 resolution ($2.81° \times 2.81°$) and 18 vertical levels in the atmosphere and used a hybrid sigma-pressure coordinate system and a time step interval of 15 minutes.

In IBIS, the geographic distribution of each plant functional type (PFT) is generated in relation to climatic variation, considering tolerance to low temperatures and degree-days requirements (Foley et al. 1996). The model determines the dominant vegetation to the grid point by the difference of the annual carbon balance resulting from different ecological strategies (Kucharik et al. 2000). IBIS incorporates 12 plant functional types (PFTs): tropical evergreen trees, tropical deciduous trees, temperate evergreen trees (broadleaf), temperate evergreen trees (conifers), temperate deciduous trees (broadleaf), boreal coniferous evergreen trees, boreal deciduous trees (broadleaf), boreal deciduous trees (coniferous), perennial shrubs, deciduous shrubs, herbaceous C3 and grasses C4.

The combination of the 12 PFTs creates the distinct ecosystems represented by the model: tropical evergreen forest, tropical deciduous forest, temperate evergreen broadleaf forest, temperate evergreen conifer forest, temperate deciduous forest, boreal evergreen forest, boreal deciduous forest, mixed forest, savanna, grassland, dense shrubland, open shrubland, tundra, desert and polar desert or ice.

Each simulation was run for 50 years, with three repetitions (ensembles) per treatment. For the control simulation observational data from global SST (http://www.cdc.noaa.gov/data/gridded/data.noaa.oisst.v2.html) and atmospheric CO_2

concentration (http:// www.esrl.noaa.gov/gmd/ccgg/trends/) for the period from 1951 to 2000 was used, with three ensembles initialized on 17-19 January 1951, to obtain a more realistic representation of vegetation and of climate situations for the same time period.

To verify the performance of the CCM3-IBIS model in simulating the regional climate during the study period in South America, the simulated precipitation is compared against six different precipitation data-bases, including two climatological surface rain gauge datasets: Climatic Research Unit (CRU; New et al. 1999), and Willmott and Matsuura (Willmott and Matsuura 2001); two that blend remote sensing data with surface rain gauges: Climate Prediction Center (CPC) Merged Analysis of Precipitation (CMAP; Xie and Arkin 1997), and Global Precipitation Climatology Project (GPCP; Huffman et al. 1997); and two reanalysis datasets: National Centers for Environmental Prediction (NCEP)–NCAR (Kalnay et al. 1996) and the 40-yr European Centre for Medium-Range Weather Forecasts (ECMWF) Re-Analysis (ERA-40) (Uppala et al. 2005).

The influence of variability in SST on vegetation cover in South America was investigated through a series of ten experimental simulations using data obtained from PCMDI (Program for Climate Model Diagnosis and Intercomparison). Ten representative coupled climate models were chosen out of those used by the IPCC in AR4 on the basis of spatial resolution and including a representative sample of meteorological research centers: CCCMA CGM3.1 T47, CNRM CM3, CSIRO MK3.0, GFDL CM2.1, GISS MODEL E_R, IPSL CM4, MIROC3.2 MEDRES, MPI ECHAM5, NCAR CCSM3.0 and UKMO HadCM3. All simulations had atmospheric concentrations of CO_2 and CH_4 in accordance with the IPCC A2 scenario. Three ensembles were conducted for all simulations, with runs starting on 17-19 January 2001. The total experiment included 1650 years of simulation.

3 Results

The monthly mean variations of precipitation simulated by CCM3-IBIS and according to the six datasets are shown in Fig. 1 for selected areas of potential vegetation (Fig. 2a) the savanna in central Brazil (cerrado), dense shrubland in northeast Brazil (caatinga) and in central Argentina (pampas). Simulated precipitation amplitude is within the amplitude of the datasets and the seasonality is well simulated too, with a slightly dry rainy season in the pampas. The performance of simulated precipitation for the Amazon tropical evergreen forest region is described in detail in a previous study (Senna et al. 2009). They found that annual mean

precipitation is within 10% of five datasets precipitation mean, and precipitation seasonality is also well simulated.

In the control simulation, the dominant vegetation of South America was simulated by the coupled model CCM3-IBIS for the period of 1991 to 2000. Since three ensembles were used, the results consist of an analysis of 30 years (10 years x 3 ensembles). If the dominant vegetation type in a given pixel is the identical in greater than 90% of the simulated years (27/30) over the three ensembles then the simulated vegetation is defined as "very robust" for that pixel; if it occurs in greater than 66% of the simulated years it is designated "robust". All other simulated vegetation (<66% of simulated years) is defined as transitional vegetation.

CCM3-IBIS provided a very robust simulation of vegetation cover over 9.3×10^6 km^2 (52%) and a robust simulation over 4.9×10^6 km^2 (27%), out of a total area of 17.9×10^6 km^2 for South America (Fig. 2). Overall, 79% of the vegetation was robustly simulated by the model, while the remaining 21% of pixels (3.7×10^6 km^2) contained transitional vegetation. The variation in dominant vegetation type does not indicate an oscillation between two radically different types of vegetation, but rather small oscillations around the condition that defines what type of PFT is dominant. This is clearly illustrated in Fig. 3 where small oscillations around the value 0.8 of leaf area index (LAI) for the pixel with coordinates 9.77°S, 45°W cause the simulated vegetation to be classified as transitional (between grassland and savanna) during the period of 1991 to 2000. IBIS specifies that a savanna ecosystem is characterized by a tree LAI of 2.5 to 0.8, while a tree LAI smaller than 0.8 characterizes a grassland ecosystem. In the case of the pixel indicated above (Fig. 3), the mean simulated tree LAI is very close to the transition point (0.8) between ecosystems (mean=0.77, n=30) – the variation being driven by the inter-annual climate variability simulated by the model. Pixels that indicate transitional vegetation represent areas in which the model is not able to generate robust predictions. The major areas of transitional vegetation (Fig. 2) are in central-western Brazil (tropical deciduous forest and savanna) and in northeastern Brazil (savanna and grasslands).

High levels of uncertainty in the forecast of dominant vegetation (2011-2050) are generated by the variability in the ten future patterns of SST (Fig. 4). Each element of Fig. 4 represents an analysis of 300 years (3 ensembles x 10 years x 10 SST). Following the same divisions outlined above, if simulated dominant vegetation is identical in more than 90% of the simulated years (>270) the results are considered "very likely" for that pixel; if it occurs in greater than 66% of the simulated years it is designated "likely". All other simulated

vegetation (<66% of simulated years) is defined as transitional vegetation where the result of the simulation is designated "uncertain".

As the simulation progresses areas of uncertainty increase (Fig. 4a-d), especially in the current border region of savanna and Amazon forest, and in northeastern Brazil, whose simulated ecosystems are predicted to vary from savanna, grassland, to open shrubland. The degree of uncertainty also increases in northern South America and in the current pampas region. In this latter region it is primarily associated with different frequencies and intensities of the El Niño event in different SST datasets: while some patterns of SST, such as the ones generated by the CSIRO and HadCM models, cause frequent and intense El Niños, other models (such as the CNRM model) generate weaker El Niño events.

In areas where the simulation produces likely and very likely forecasts various biogeographical trends can be discerned. One of the clearest patterns is the wide-scale replacement of savanna by tropical deciduous forest that can be seen experimental simulations (Fig. 4e-l). The other major ecosystem types of South America do not show significant spatial changes in experimental simulations (Fig. 4e-l).

The simulated trends in geographic coverage the results considered robust/very robust and likely/very likely (i.e. analysis of grid points above 66% occurrence of vegetation) for the five major ecosystems in South America (1991-2050) show a complex pattern of change and replacement that is subject to sharply increasing levels of uncertainty (Fig. 5). The area of transition vegetation from the control simulation (3.7×10^6 km²) is filtered for the entire period 2001-2050, and it is not represented in Fig. 5. With the exception of tropical deciduous forest, all the major ecosystem types were characterized by a reduction in predicted area over the course of the simulation: savanna (predicted reduction =2.7×10^6 km²), grassland (=1.1×10^6 km²), tropical evergreen forest (=0.67×10^6 km²) and temperate evergreen broadleaf forest (=0.1×10^6 km²). These reductions in absolute area were accompanied by an increase of 5×10^6 km^2 of areas where the coupled-model ensemble was unable to give a robust prediction about the type of ecosystem within a grid square. Most notably, from the perspective of international conservation, the absolute area of tropical evergreen forest in Amazonia is predicted to decline by as much as 18% by the 2040s – although, as with the other predicted declines, the actual figure may be lower due the increasing levels of uncertainty generated by the simulations.

4 Discussion

The results of the simulations point to an increasing degree of uncertainty associated with predictions for South American vegetation over the next forty years of the current century. Using the latest data and modeling techniques it is impossible to predict, with a greater than 66% chance of success, the vegetation cover in areas equivalent to 28% of South America (5×10^6 km^2). However, it is important to note that this uncertainty is not evenly distributed throughout the continent and that there are important and robust predictions concerning redistributions of major vegetation types. These "areas of uncertainty" include parts of eastern Amazonia, northeast Brazil and northern South America (Guyana/Venezuela). The range of climate uncertainty (in precipitation and temperature for example) that goes into the vegetation modeling is expected to be smaller than the range of uncertainty found in climate predictions from different GCMs, as vegetation response depends mainly on the combination of temperature and precipitation changes and such combination tends to be the same for the same GCM. The use of a single climate model reduced the level of climate model related uncertainty.

The source of the uncertainty in the reported simulations is mainly attributable to the variability in the ten simulated patterns of SST which are influencing the complex dynamics of the interaction between the regional climate and the dominant vegetation cover. Predictably, the first areas to be affected by this uncertainty are those that are currently classified as transitional vegetation. As the simulation progresses and the SST scenarios diverge, such transitional areas expand, eventually leading to large swathes of uncertainty spreading over vast areas of the north and northeast of the continent. The significance of this uncertainty is that in areas such as northeastern Brazil the predicted ecological end-points may range from savanna, grassland and open shrubland. This uncertainty provides a significant socio-economic and conservation challenge to planners and policy makers and is a stark warning against ascribing too much weight to the results of any of the existing simulations that forecast vegetation cover in this region.

Uncertainty in predicting future vegetation coverage has been found in other modeling studies, albeit at a much cruder scale. Alo and Wang (2008) examined the geographical responses of natural vegetation to future changes in atmospheric CO_2 concentration and climate at a global level. To achieve this they used an offline version of the National Center for Atmospheric Research Community Land Model's (NCAR CLM) dynamic global vegetation model, forced by the climate simulated by eight general circulation models. The

eight simulations showed a great deal of uncertainty, especially with respect to the coverage of evergreen trees in South America with some models predicting dieback while others predicted enhancements in forest cover in some regions.

However, despite the uncertainty our study also indicates that some areas are likely to change (or remain unchanged) whatever SST scenario is used. Among these robust forecasts the most striking is the expansion of tropical deciduous forest from its current distribution centered in the State of São Paulo, to occupy a large part of central Brazil by 2050. One explanation for this expansion is the fertilization effect that is predicted to be mirrored by a reduction of the cerrado vegetation that currently predominates in this region. Lapola et al. (2009) show that if, in the future, CO_2 fertilization effect does not play any role in tropical ecosystems then there must be substantial biome shifts in the region, including substitution of the Amazonian forest by savanna. Otherwise, if CO_2 fertilization indeed enhances NPP in the future, then impacts could be less catastrophic, while most of Amazonia would remain the same. They also found small area of uncertainty in southeast Amazonia associated with uncertainties in future precipitation anomalies.

Our results also show the hotly debated Amazon region possesses a core area in the west that is predicted to remain unchanged across the range of SST used in the simulation. The risk of Amazon forest dieback in northwestern Amazonia is almost eliminated if the direct impacts of CO_2 on plant productivity and water-use efficiency are great (Rammig et al. 2010). However, overall 18% of the tropical evergreen forest in Amazonia is considered area uncertain, predicted to be replaced by tropical deciduous forest or savanna (or may even remain as tropical evergreen forest) by 2050. This result is in general concordance with other regional modeling studies (e.g. Cox et al. 2000, 2004; Salazar et al. 2007; Cook and Vizy 2008) although, as would be anticipated given the uncertainties involved, these vary considerably. For example, Salazar et al. (2007) estimated a 9% reduction in Amazon forest cover during the period 2050–2059 for the A2 emission scenario, when at least 75% of the calculations agree on the projecting biome change (consensus), while Cook and Vizy (2008) predicted an enormous 69% reduction by 2100 using an asynchronous coupling between the regional climate model (MM5 RCM) and the potential vegetation model (CPTEC-PVM). Rammig et al. (2010) concluded that the uncertainty associated with the long-tern effect of CO_2 is much larger than that associated with precipitation change, and this underlines the importance of reducing uncertainties in the direct effects of CO_2 on tropical ecosystems.

5 Conclusions

Accurate forecasting of vegetation patterns under climate change at a regional or global scale in response to expected increases in CO_2 is a vital prerequisite for effective land use planning, adaptation and mitigation measures. However, such complex simulations inevitably generate large uncertainties, especially where small changes in simulated climate can lead to major ecosystem transitions. Understanding the nature and extent of these uncertainties, and geographically locating areas for which the best forecasts are inherently uncertain is thus an important objective for the international modeling community.

The current study is an important first step in highlighting and estimating some of the uncertainties associated with this process of environmental forecasting in South America. Our quantitative assessments, based on the patterns of predicted SST, show a complex set of future determinations of vegetation patterns in South America. Sorting between these alternative scenarios will require the development of new mathematical and statistical tools that provide not only estimates on the climate impact, but which also better quantify the uncertainties involved.

Acknowledgments We acknowledge the financial support by the Amazonas and Minas Gerais State Research Funding Agencies (FAPEAM, FAPEMIG). The paper was read and edited by Dr Richard Ladle, Oxford University.

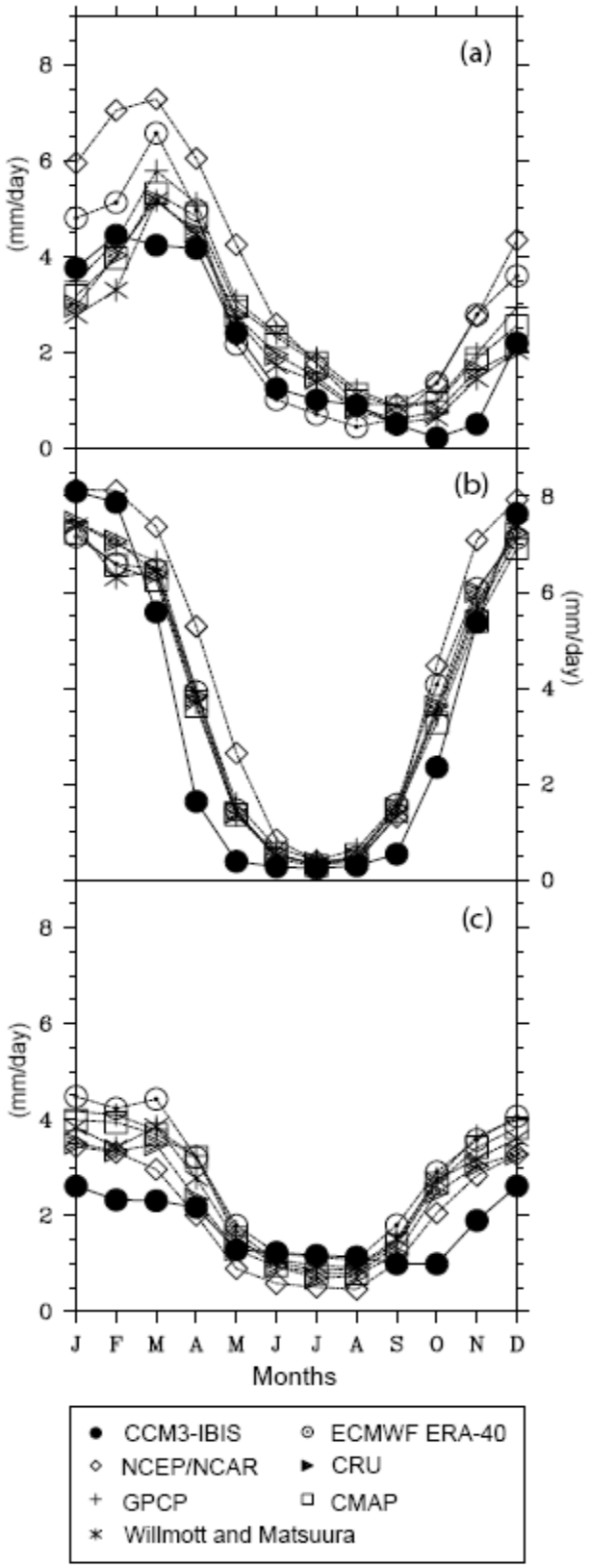

Fig. 1 Monthly variation of precipitation for the caatinga (a), cerrado (b) and pampas (c) region.

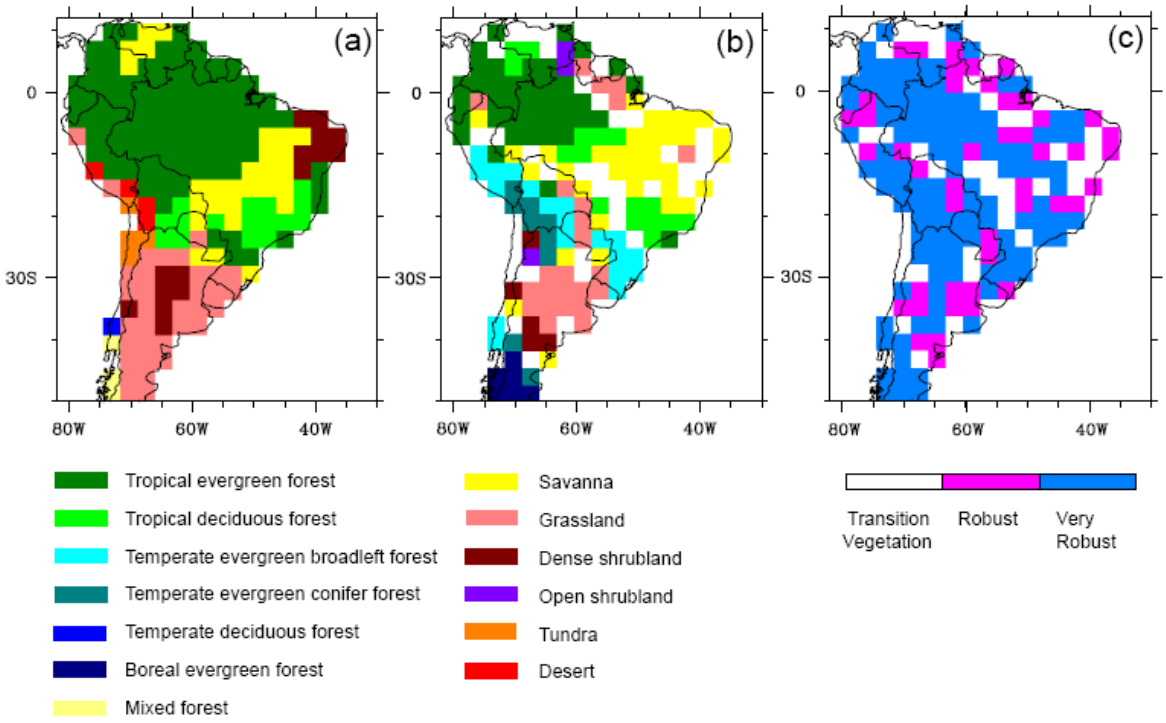

Fig. 2 Panels (a) illustrate results the potential vegetation. Panels (b-c) illustrate results of the control simulation, where panel (b) shows simulated pattern of dominant vegetation for the period of 1991-2000, and panel (c) shows robustness of the control simulation (see text for details).

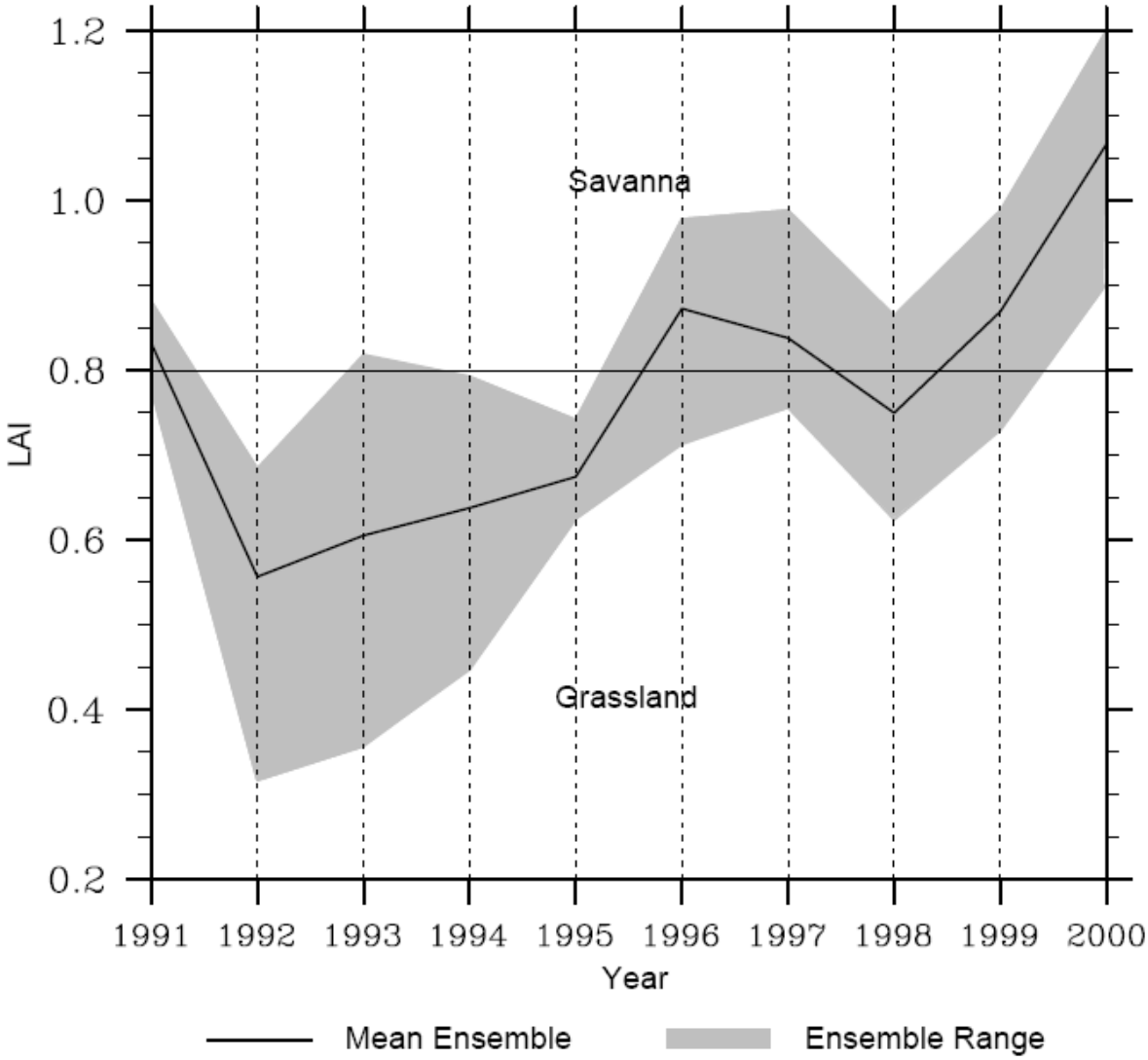

Fig. 3 Tropical trees leaf area index ensemble range and mean for the pixel (9.77°S, 45°W) for the period of 1991 to 2000. Note that during the period 1996-1999 the simulations vary considerably in whether they predict grassland or savanna.

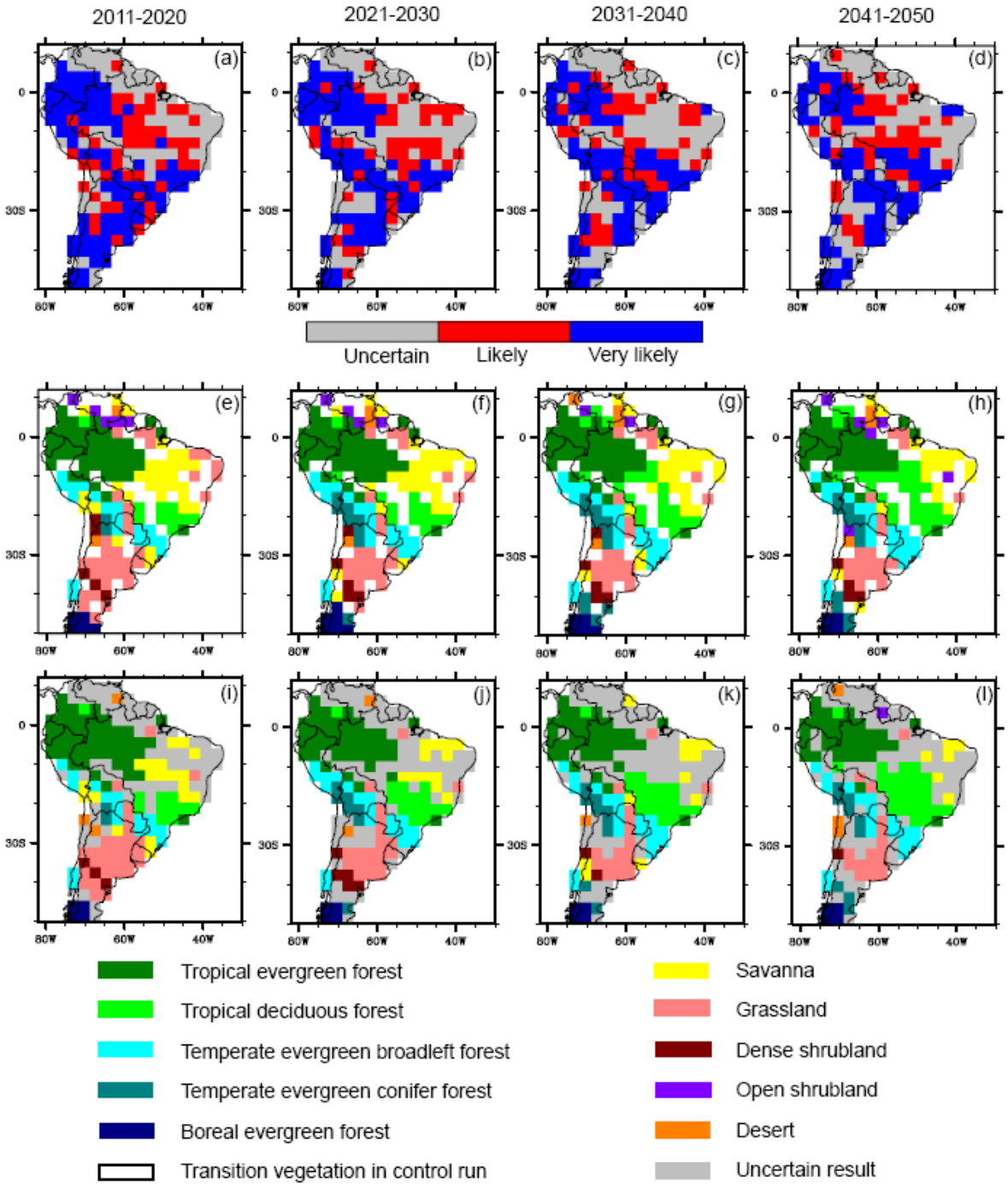

Fig. 4 Panels (a-l) illustrate forecast vegetation cover in South America 2011-2050 based on increased CO_2 atmospheric concentration for the A2 scenario of IPCC, where panels (a-d) show the overall uncertainty levels of each pixel (see text for details), and panels (e-l) illustrate the results of the experimental simulations using 10 different estimates of SST. In addition panels (e-h) illustrate the transition vegetation in control run in white, and panels (i-l) illustrate the uncertain results in gray.

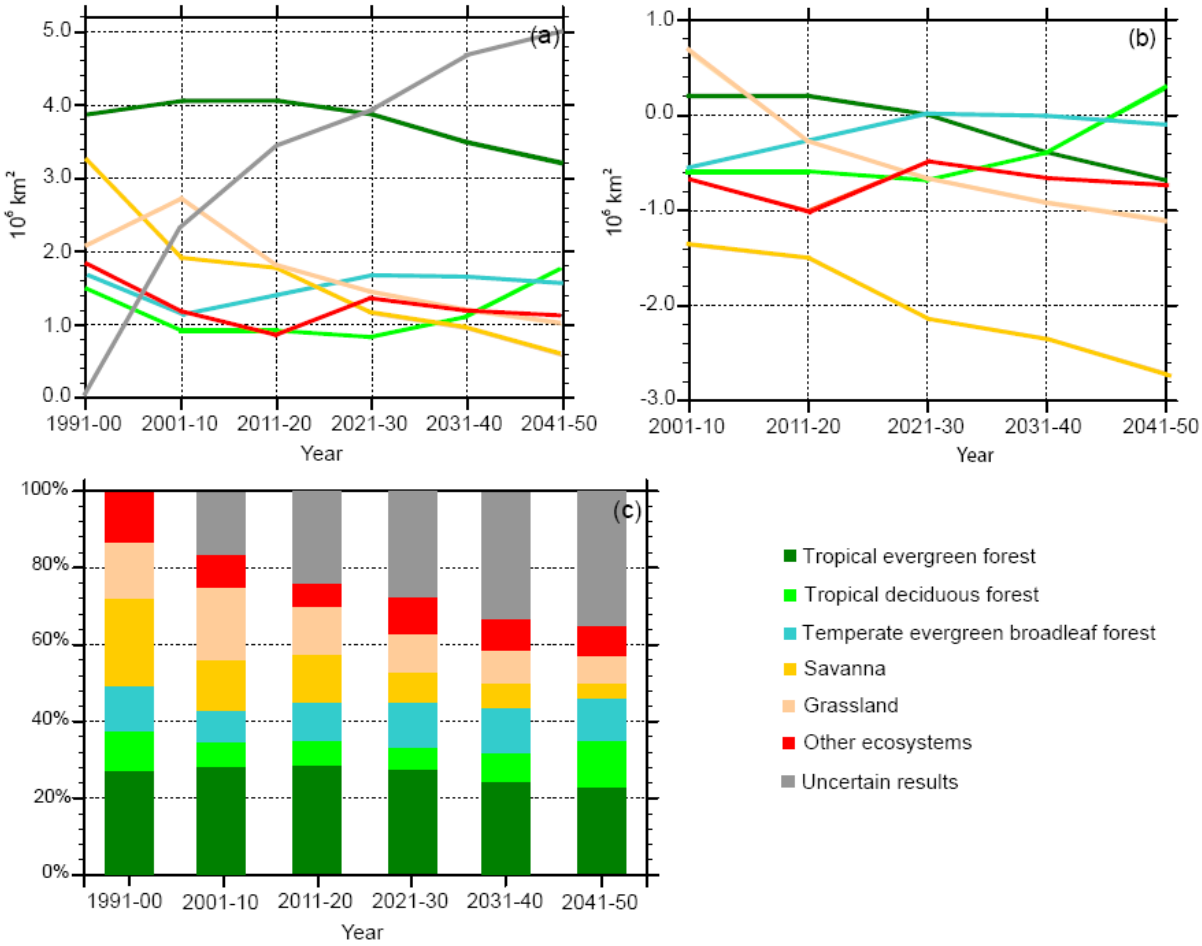

Fig. 5 (a) Area occupied by the five major ecosystems in South America for the grid points considered robust/very robust in the control simulation (1991-2050). (b) Change in area occupied by different vegetation types (2001-2050) as compared to reference period (1991-2000). (c) Percentage area occupied by the five major ecosystems for the grid points considered robust/very robust in the control simulation (1991-2050).

Capítulo 2

Pereira, M. P. S., M. H. Costa, F. Justino, and A. C. M. Malhado, **Response of South American terrestrial ecosystem to future patterns of Sea Surface Temperature.** Manuscript to be submitted to Journal of Geophysical Research – Biogeosciences.

Abstract

Global warming in the first half of the 21th century is likely to have profound influences on South American vegetation and climate. Although various models exist that seek to model the dynamic interactions between vegetation types and climate under scenarios of global warming, such coupled models have not been used to assess the potentially critical role of variations in sea surface temperature (SST) in modifying the climate-vegetation interactions across the continent. Here, we use monthly output of a 100-year coupled model run to investigate how South American vegetation will respond to future patterns of SST in the Pacific and Atlantic, under a global warming scenario. Specifically, we assess statistical correlations between SST variability and vegetation in six different South America regions. The results demonstrate that the model provides a robust simulation of changes in mean precipitation, net primary production (NPP), upper canopy leaf area index (LAI) and lower canopy LAI under warming and non-warming scenarios. Most significantly, spatial-temporal variability in SST exerts a strong influence over the vegetation dynamics in all six South American regions. However, there was considerable variation in the direction and magnitude of SST effects in different regions. We conclude that accurate and robust analysis of the South American climate and associated vegetation dynamics under global warming need to consider the SST pattern.

1. Introduction

The Intergovernmental Panel on Climate Change (IPCC) estimates that global mean surface temperatures have increased by 0.74°C ± 0.18°C over the last 100 years (1906-2005), the rate of warming over the last 50 years being almost double that over the last 100 years

(0.13°C ± 0.03°C vs. 0.07 ± 0.02°C per decade) (Trenberth et al., 2007). Most of the observed increase in global average temperatures since the mid-20th century is very likely due to increases in anthropogenic greenhouse gas concentrations (Hegerl et al., 2007).

Global warming will have dramatic impacts on ecosystems and the species that inhabit them (e.g. Thomas et al., 2004), and it is therefore vitally important that scientists are able to develop robust models that are able to realistically capture the complex and dynamic relationship between the climate and land use. The response of vegetation in South America to climate change may be particularly important as this continent still contains the largest (but rapidly diminishing) continuous area of tropical rainforest. The potential impacts of climate change on this and other South American ecosystems are currently poorly understood, as is the role of these ecosystems may play in determining the extent and geographical pattern of the changing climate.

There are several current models that simulate the dynamic relationship between climate and vegetation at a macrogeographic scale (Levis et al., 2000; Cox et al., 2004; Betts et al., 2004; O'ishi and Abe-Ouchi, 2009). These could be of great utility for climate modelers since, unlike many climate simulations, they consider the atmosphere and terrestrial biosphere as a coupled system with biogeophysical and biogeochemical processes occurring across a range of timescales (Foley et al., 2000). Specifically, when a dynamic model is coupled to an atmospheric general circulation model it is possible to investigate the influence of vegetation dynamics on climate change under conditions of global warming (O'ishi and Abe-Ouchi, 2009).

The results from such coupled models predict that one of the impacts of doubled/quadrupled CO_2 in the Amazon region will be an increase in CO_2 fertilization which could counteract the potential decrease in net primary production (NPP) associated with warming (O'ishi and Abe-Ouchi, 2009 - similar results obtained by Cox et al., 2000, 2004; Betts et al., 2004). However, these results are strongly in contrast with other coupled model numerical studies on the response of tropical vegetation elevated CO_2. Moreover, the simulations indicated that an increase in CO_2 will be accompanied by an increase in vegetation cover in tropical regions: this process would initiate a feedback loop through the hydrological cycle, leading to an increase in precipitation and soil moisture (Levis et al., 2000).

The conflicting results may be due, in part, to the influence of different patterns of sea surface temperature (SST) used by the coupled simulations, since the South American climate is strongly dependent on the patterns of SST in the Pacific and Atlantic (Nobre and Shukla,

1996; Diaz et al., 1998; Grimm et al., 2000; Haylock et al., 2006). Such changes in climate will have knock-on effects on vegetation. For example, when a coupled climate-vegetation model was forced by future SST and sea ice (projected with 17 atmosphere–ocean general circulation models participating in the IPCC Fourth Assessment Report, and by appropriate atmospheric carbon dioxide concentrations under the A2 emission scenario) (Jiang et al., 2011), vegetation was predicted to become denser (in terms of increases of global mean leaf area index).

Although several studies using coupled models have already investigated the effects of vegetation feedback under global warming (see above), they are either restricted to particular parts of South America such as the Amazon or do not take into account the behavior of vegetation in relation to SST variability. Thus, the objective of the present study is to use a coupled climate-vegetation model (a 100-year monthly model CCM3-IBIS running from 1951 to 2050) to evaluate the influence of spatial-temporal variability in SST on South American vegetation dynamics under global warming.

This study seeks to answer to the following fundamental questions:

- How will the vegetation of South America respond to future patterns of SST in the Pacific and Atlantic?
- What correlations exist between the SST variability and vegetation characteristics in different South America regions?

The paper is organized as follows. First, we provide a concise overview of the model, including processing schemes, details of the initial state spin-up, simulation setting, and forcing data. Second, we analyze the simulation results and discuss the accuracy of the model simulation, the predicted response of South American terrestrial ecosystems to global warming in first half of 21th century, and the influence of ocean surface patterns in the South America ecosystem variables. Finally, we provide concluding remarks on the efficacy and validity of the study.

2. Model Description and Experiment Design

Experiments are performed using the National Center for Atmospheric Research (NCAR) Community Climate Model Version 3 (CCM3) (Kiehl et al., 1998) with spatial resolution T42 (2.81° x 2.81°), 18 vertical levels in the atmosphere, and using a hybrid sigma-pressure coordinate system and a time step interval of 15 minutes. This model is coupled with an updated version of the surface model known as the Integrated Biosphere Simulator (IBIS) (Foley et al., 1996). IBIS is a dynamic global vegetation model which considers changes in

the composition and structure of vegetation in response to environmental conditions (detailed specification in Delire et al., 2002).

Most significantly, IBIS provides a representation of vegetation dynamics appropriate for global ecosystem modeling. NPP is calculated by integrating primary production through the year discounting maintenance respiration and the carbon lost due to growth respiration. Leaf area index (LAI) is simulated according to climatic conditions such as temperature, precipitation and plant productivity, which in turn depend on LAI. In each grid cell of the model a number of plant functional types (PFT) can exist simultaneously. Competition among PFTs is characterized by the ability of plants to capture common resources (light and water). For example, light is first captured by the LAI of PFTs in the upper canopy and therefore less light is available for the lower canopy. However, lower canopy LAI has primary access to soil moisture as it infiltrates through the soil (Foley et al., 1996). Competition between PFTs in the same layer of the canopy is represented by the difference of the annual carbon balance resulting from different ecological strategies (Kucharik et al., 2000).

A set of simulations is designed to generate a detailed view of patterns of SST related vegetation patterns over South America. We conduct two groups of simulations: (1) a control simulation for the second half of the 20th century that assumes present-day conditions, and; (2) a series of ten experimental simulations for future climate scenarios for the first half of the 21th century. Each simulation is run for 50 years, with three repetitions (ensembles) per group of simulations.

The control simulation uses observational data from global SST (http://www.cdc.noaa.gov/data/gridded/data.noaa.oisst.v2.html) and atmospheric CO_2 concentration (http:// www.esrl.noaa.gov/gmd/ccgg/trends/) for the period from 1951 to 2000. To obtain a more realistic representation of vegetation and climate scenarios for the same time period, the control simulation uses three ensembles initialized on 17-19 January 1951.

The series of ten experimental simulations use data from global SST obtained from PCMDI (Program for Climate Model Diagnosis and Intercomparison). Ten representative coupled climate models are chosen (out of those used by the IPCC in AR4) on the basis of spatial resolution and include a representative sample of meteorological research centers: CCCMA CGM3.1 T47, CNRM CM3, CSIRO MK3.0, GFDL CM2.1, GISS MODEL E_R, IPSL CM4, MIROC3.2 MEDRES, MPI ECHAM5, NCAR CCSM3.0 and UKMO HadCM3. All simulations have atmospheric concentrations of CO_2 and CH_4 in accordance with the IPCC A2 scenario. Three ensembles are conducted for all simulations, with runs starting on 17-19 January 2001. The total experiment includes 1650 years of simulation.

The performance of the CCM3-IBIS model in simulating the regional climate during the control period in South America is verified by a comparison of the simulated precipitation against six different precipitation databases. These databases include two climatological surface rain gauge datasets (Climatic Research Unit (CRU; New et al., 1999), and Willmott and Matsuura (Willmott and Matsuura, 2001)), two that blend remote sensing data with surface rain gauges (Climate Prediction Center (CPC) Merged Analysis of Precipitation (CMAP; Xie and Arkin, 1997), and Global Precipitation Climatology Project (GPCP; Huffman et al., 1997)), and two reanalysis datasets (National Centers for Environmental Prediction (NCEP)–NCAR (Kalnay et al., 1996) and the 40-yr European Centre for Medium-Range Weather Forecasts (ECMWF) Re-Analysis (ERA-40) (Uppala et al., 2005)).

The study is conducted for six regions over South America: Northern South America (NSA), with coordinates on land of 0° to 10°N by 60°W to 77°W; Western Amazonia (WA) within 2°N to 9°S and 63°W to 80°W; Eastern Amazonia (EA) within 2°N to 9°S and 49°W to 62°W; Northeast Brazil (NEB) within 2°S to 18°S and 36°W to 48°W; Central Brazil (CB) within 10°S to 26°S and 49°W to 62°W; Patagonia (PA) within 28°S to 49°S and 56°W to 68°W (Figure 1).

3. Results and Discussion

The large size of continental South America means that the climate and vegetation varies considerably on a regional basis. For example, there is great regional variability in the seasonal cycle of precipitation (see grid-cells indicated in Figure 1). Specifically, the NSA, WA and EA regions show high precipitation values while the NEB, CB and PA regions show lower precipitation values. Simulated precipitation amplitude is within the amplitude of the datasets, and seasonality is also well simulated with a delayed rainy season in the NSA and before the dry season in the WA. The simulated precipitation for the Amazon tropical evergreen forest region has been described in detail in a previous study (Senna et al., 2009), which found that annual mean precipitation was within 10% of the precipitation mean of five datasets, and that precipitation seasonality was also well simulated.

In the first half of 21th century (2041-2050), climate conditions simulated by CCM3-IBIS model in response to increased greenhouse gases in South America differ from the baseline (1991-2000) climate (Figure 2). A mean decadal precipitation increase in WA region and decrease in NSA region is obtained in the period 2041-2050 as compared to the reference period 1991-2000 (Figure 2a-2c). These differences in precipitation are characteristic in South America precipitation anomalies during El Niño events (Aceituno et al., 2009). The future

NPP scenario (2041-2050) shows an increase across almost all areas of South America due to elevated atmospheric CO_2 – the CO_2 fertilization effect. The vegetation becomes more productive over WA (Figure 2d-2f). Such a change in carbon assimilation is mainly due to precipitation increases in the region. Future climate conditions are observed to produce a simultaneous increase in the LAI upper canopy in all areas of South America, except NSA (Figure 2g-2i), as a consequence of the physiological effect of raised CO_2. Lower canopy LAI is observed over the PA region, where grassland vegetation predominates. In contrast, upper canopy lower canopy LAI show positive trends over the NEB region and negative trends in the NSA region (Figure 2j-2l).

The coefficient of variation (the ratio of the standard deviation to the mean as a measure of relative variability) provides a useful tool to compare the decadal variability of present-day conditions (1991-2000) and future scenario (2041-2050) simulations in the context of mean precipitation, NPP, upper canopy LAI and lower canopy LAI (Figure 3). The largest coefficient of variation is found in the future decadal (2041-2050) scenario which is also characterized by a large standard deviation. This increase is attributable to the variability in the ten future patterns of SST - an analysis of 300 years (3 ensembles x 10 years x 10 SSTs). It should be noted that, in contrast, the present-day conditions simulation only consists of an analysis of 30 years (3 ensembles x 10 years x 1 SST).

Some changes in vegetation cover in South America during 1991-2000 and 2041-2050 are also forecast (Figure 4). One of the clearest changes in vegetation structure is the replacement of savanna by tropical deciduous forest. The distribution of other major South American ecosystem types does not show large changes in the experimental simulations. Jiang et al. (2011) also observed that increases of deciduous forest will be one of the main characteristics of the changes in vegetation composition under future global warming.

The relationship between SST and the diverse patterns of South American vegetation can be best addressed through a statistical analysis of the patterns of variability. The spatial variation in the SST is based on a series of bi-dimensional correlations between the 10 future patterns of the SST and the precipitation data, NPP, upper canopy LAI and lower canopy LAI – estimated from the different SST scenarios for 2011-2050. These data are analyzed for 400 years (40 years x 10 SST scenarios) for all six regions (Figures 5-10). The correlation between the mean spatial variation for each region and SST for each point on the grid is assessed under the influence of global warming scenarios (Figures 5a-5d – 10a-10d) and with the warming trend removed (Figures 5e-5h – 10e-10h).

Precipitation, NPP and LAI upper canopy over the NSA region are negatively correlated with SSTs in the equatorial Pacific and Atlantic oceans (Figure 5a-5c). The northern hemisphere plays an important role in inducing positive precipitation anomalies in the equatorial zone of the tropical and subtropical Atlantic. This result agrees with those of Marengo et al. (2005). Increases in SST over this region induce a northward position of the Intertropical Convergence Zone (ITCZ) associated with changes in the meridional gradient of atmospheric pressure. Under this scenario increased precipitation would be induced in the NSA. It is important to highlight that statistically significant correlations are generated in the western Pacific, along the coast of Japan, and near the west coast of South America. This pattern is very similar to the warm phase of the Pacific Decadal Oscillation (PDO). However, the correlation between lower canopy LAI and SST is in strong contrast to the previous patterns - in the sense that there is a positive correlation in the equatorial region of both Atlantic and Pacific Oceans, and negative correlation elsewhere, which may resemble the cool phase of the PDO (Figure 5d).

When the linear global warming trend is removed the largest correlation between precipitation and SST over the NSA is located in the equatorial region. Thus, La Niña years induce positive precipitation anomalies (Figure 5e). This is partially reproduced by the NPP (Figure 5f), although changes in NNP and upper canopy LAI (Figure 5g) are also influenced by the warmer subtropical Pacific. Lower canopy LAI is more highly correlated with the colder equatorial Pacific as reproduced by the precipitation anomalies (Figure 5h, 5e).

In the case of WA region, there is a positive correlation between precipitation, NPP, upper canopy LAI and SSTs in large parts of the Pacific and Atlantic oceans (Figure 6a-6c). This suggests there is no substantial dependence of the WA climate-vegetation patterns on the equatorial Pacific climate variability under global warming conditions (i.e. the global effect of higher SSTs is dominant). However, in the case of lower canopy LAI, equatorial SSTs seem to play an important role in defining the pattern of change (Figure 6d). These results differ from those predicted to occur for the NSA region. In the absence of global warming the equatorial Pacific is highly correlated with the WA region for both precipitation and NPP, whereas it does not strongly affect upper canopy LAI which exhibits a higher correlation with the Southern Hemisphere (SH) SSTs (Figure 6e-6g). It is interesting that the WA region is statistically correlated with the subtropical Atlantic Ocean, perhaps due to the influence of the South Atlantic Convergence Zone (SACZ). However, there is no statistically significant correlation for lower canopy LAI (Figure 6h).

The SST correlation with rainfall, NPP and upper canopy LAI in the EA region under global warming conditions shows a similar pattern to that of the WA region (Figure 7a-7c). Lower canopy LAI shows a negative correlation (Figure 7d). Although the equatorial Pacific plays a significant role to defining the precipitation pattern in EA region, this is not reflected in terms of NPP and upper canopy LAI, which are more influenced by the subtropical Pacific Ocean. The tropical Atlantic Ocean should arguably also be included as a driver of the vegetation-climate interaction in the EA region, in particular for upper canopy LAI (Figure 7).

The NEB region (Figure 8) is dominated by two biomes with distinct characteristics: the "Mata Atlantica" or Atlantic forest is a region of tropical dry forest and tropical savanna. The second biome is the Caatinga, which extends into the interior of northeastern Brazil. This biome is characterized by a xeric shrubland and sparse forests of small, thorny trees that changes their leaves seasonally. Caatinga is a unique biome because, despite being located in an area (northeast Brazil) dominated by semi-arid conditions, it shows great variety of biologically diverse landscapes and a high degree of endemism.

There is a negative correlation between the equatorial Pacific SST and precipitation in the NEB region (Figure 8). This is anticipated since SST changes in this oceanic region induce modifications in the Walker circulation leading to air subsidence in the NEB region (Grimm et al., 2003). On the other hand, positive correlations are noted with the subtropical Pacific and SH tropical Atlantic (Figure 8a). Positive SST anomalies in the tropical south Atlantic are associated with a dominance of negative surface pressure anomalies and therefore with a southward migration of the ITCZ. Such a migration may lead to positive precipitation anomalies - as is predicted to occur. Moreover, it should be noted that the negative correlation in the tropical north Atlantic reinforces the austral displacement of the ITCZ (Figure 8a). The results for NPP and upper canopy LAI are quite similar, with a negative trend on the tropical Pacific and tropical North Atlantic, and a positive trend in extratropical oceans (Figure 8b, 8c). Lower canopy LAI gives an inverse signal to that of precipitation, NPP and upper canopy LAI (Figure 8d).

In the absence of global warming, precipitation in the NEB region shows a negative correlation with equatorial Pacific SSTs, which is directly related to the ENSO – when the SST is higher than normal there is a decrease in precipitation over the NEB region (Figure 8e). However, the equatorial Pacific does not seem to induce substantial modifications in NPP and upper canopy LAI characteristics. The NPP has a positive correlation with subtropical South Pacific and tropical Atlantic SSTs (Figure 8f). Upper canopy LAI is correlated with positive values of SST anomalies in most parts of the ocean basins, in particular with the

subtropical Pacific along the 30S latitude belt (Figure 8g). Lower canopy LAI is negatively correlated with global SST (Figure 8h).

There is also a clear link between SST and vegetation-climate in the central part of South America, which is primarily dominated by Savanna. Most noticeably, there are several similarities in the correlation distribution for precipitation, NPP and upper canopy LAI (Figure 9a-9c). However, once again these patterns do not match with those predicted for lower canopy LAI (Figure 9d). When the effect of global warming is removed, precipitation in the CB region is positively correlated with equatorial Pacific SSTs (Figure 9e). Analysis of NPP demonstrated a positive correlation with SST in the Tropical Pacific, and the Tropical Atlantic (Figure 9f). Upper canopy LAI is statistically correlated with SST over most oceanic basins, with a higher index in the south extratropical Pacific (Figure 9g). Lower canopy LAI is negatively correlated with subtropical South Pacific and Atlantic SSTs (Figure 9h).

The climate of the southern South America region (including Patagonia) is tightly dependent on SST changes in the extropics, and is also correlated with the equatorial Pacific (Figure 10). The influence of extratropical SSTs may play a leading role in influencing precipitation, NPP, and both upper and lower canopy LAI. However, in the case of precipitation and lower canopy LAI some response to the eastern subtropical northern Pacific is also observed. Under of the no global warming scenario, precipitation and NPP are strongly influenced by the equatorial Pacific, and upper canopy LAI is influenced by the global pattern of SST. Lower canopy LAI is mainly driven by the subtropical southern Pacific (Figure 10h).

4. Conclusions

The results of this study, using the CCM3-IBIS coupled model clearly demonstrate the significant influence that SST may play in the future dynamics of South American terrestrial ecosystems. Our quantification of the potential changes in natural vegetation under global warming in first half of 21th century predict an increase in high-productive vegetation due to the effect of atmospheric CO_2 fertilization. In general, the increased atmospheric CO_2 emissions will be accompanied by changes in precipitation, with a high possibility of weather conditions causing noticeable changes in regional vegetation composition and structure. CO_2 enrichment is predicted to stimulate NPP in most South American ecosystems vegetation becoming denser through increases in upper canopy LAI – particularly in the Brazilian Cerrado region where the vegetation structure will undergo noticeable changes as it is replaced by tropical deciduous forest. It is also clear from the no warming scenario that there are dependencies on SST patterns in the coupled atmosphere-biosphere system of all six

South American regions. In conclusion, at a macrogeographic scale changes in SST in the Atlantic and Pacific oceans are an important driver of changes in the structure of the South American vegetation.

The effect of future climate change on South America such as forest fires, storms, severe droughts, and increased/decreased vegetation productivity, will command public attention and place increasing demands on management resources. Increased utilization of sophisticated and appropriately parameterized models (dynamic climate-vegetation, controlled SSTs) will provide a more realistic picture of the identity and relative importance of the main drivers of vegetation change under climate change. The results presented here strongly indicate the need for further investigation into the role of SST patterns on vegetation (and terrestrial ecosystem in general). Future research should focus on further elucidating the nature of complex ocean-atmosphere-biosphere interactions and there impacts on the macrogeographic distribution of vegetation and on climate variability. More specifically, an important step towards this goal would be additional analyses that link changes in PFT within ecosystems to specific patterns of SST.

Acknowledgments. We thank Amazonas and Minas Gerais State Research Funding Agencies (FAPEAM, FAPEMIG) for financial support. We also thank Dr. Richard J. Ladle for reviewing the English and commenting on the manuscript.

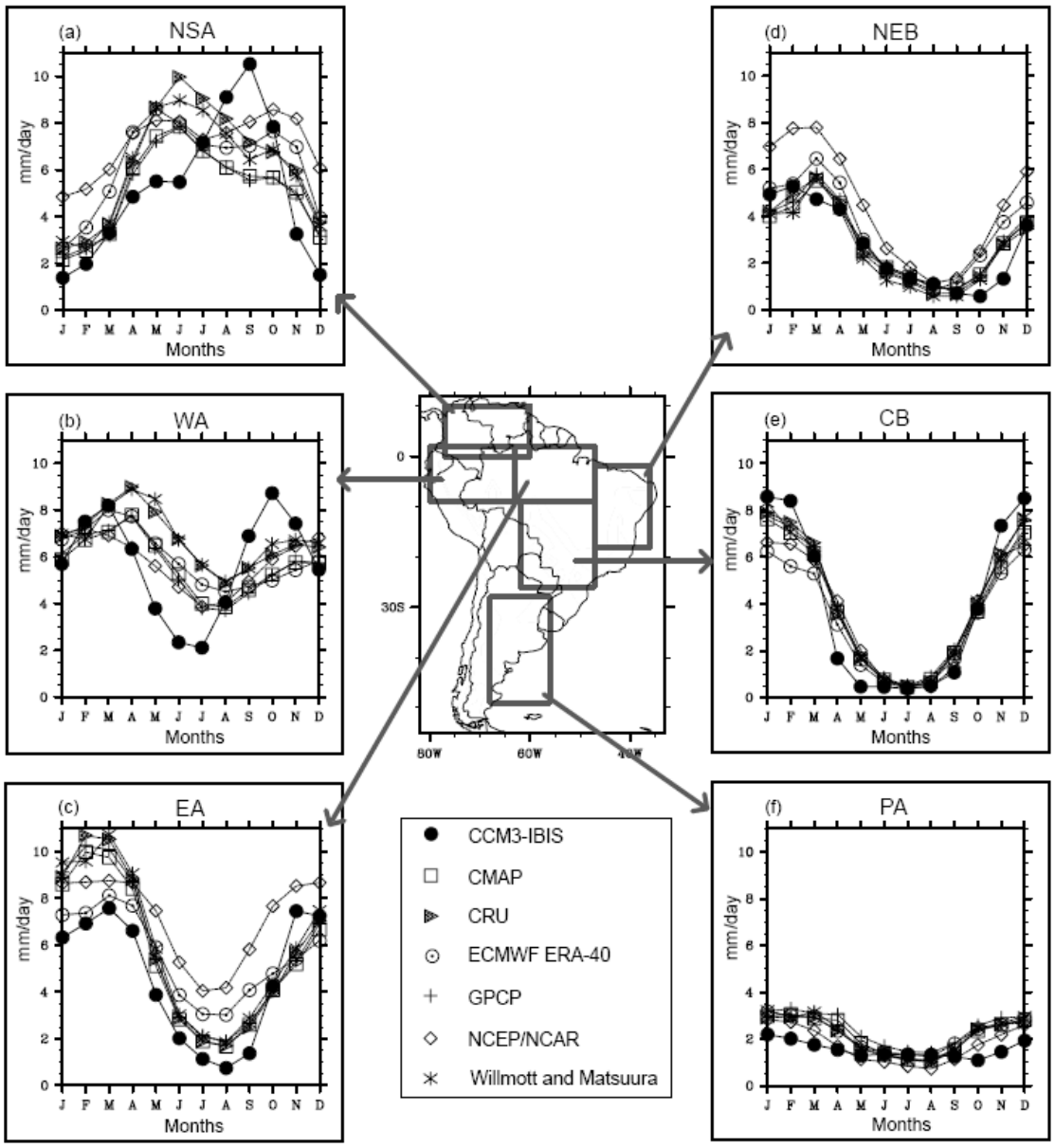

Figure 1 – Seasonal cycle of precipitation climatology for the NSA (a), WA (b), EA (c), NB (d), CB (e) and PA (f). Individual data sources (various markers; see legend). Boxes indicate the regions as defined for this analysis.

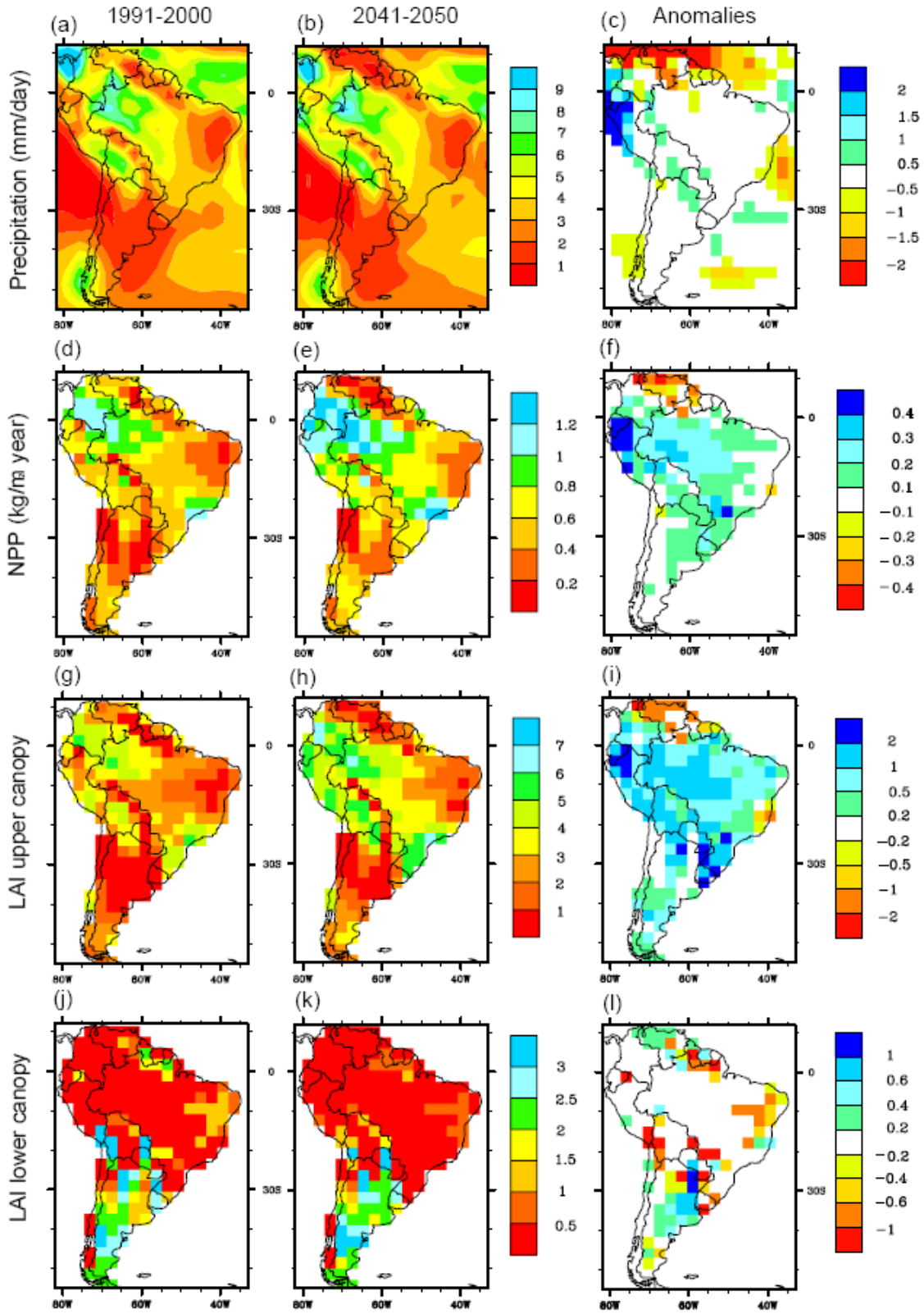

Figure 2 – Mean decade of precipitation (mm/day) (a-b), NPP (kg/m²year) (d-e), LAI upper canopy (m²/m²) (g-h), and LAI lower canopy (m²/m²) (j-k) in South America, over present-day conditions (1991-2000) (a, d, g, j) and future scenario (2041-2050) (b, e, h, k), and anomalies (2041-2050 – 1991-2000) (c, f, I, l).

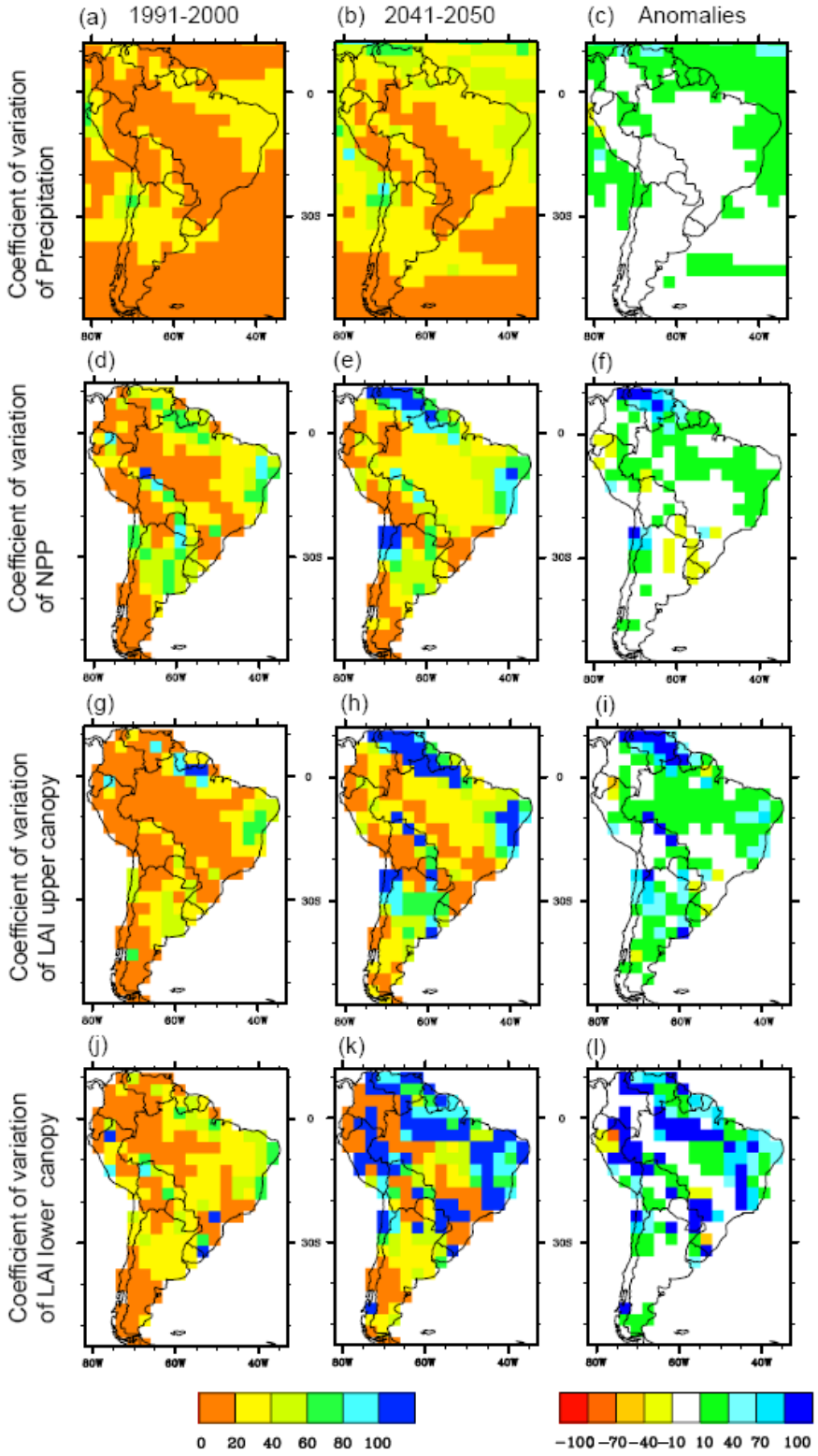

Figure 3 – Coefficient of variation of precipitation (a-b), the NPP (d-e), upper canopy LAI (g-h) and lower canopy LAI (j-k) in South America, over present-day conditions (1991-2000) (a, d, g, j) and future scenario (2041-2050) (b, e, h, k), and anomalies (2041-2050 – 1991-2000) (c, f, I, l).

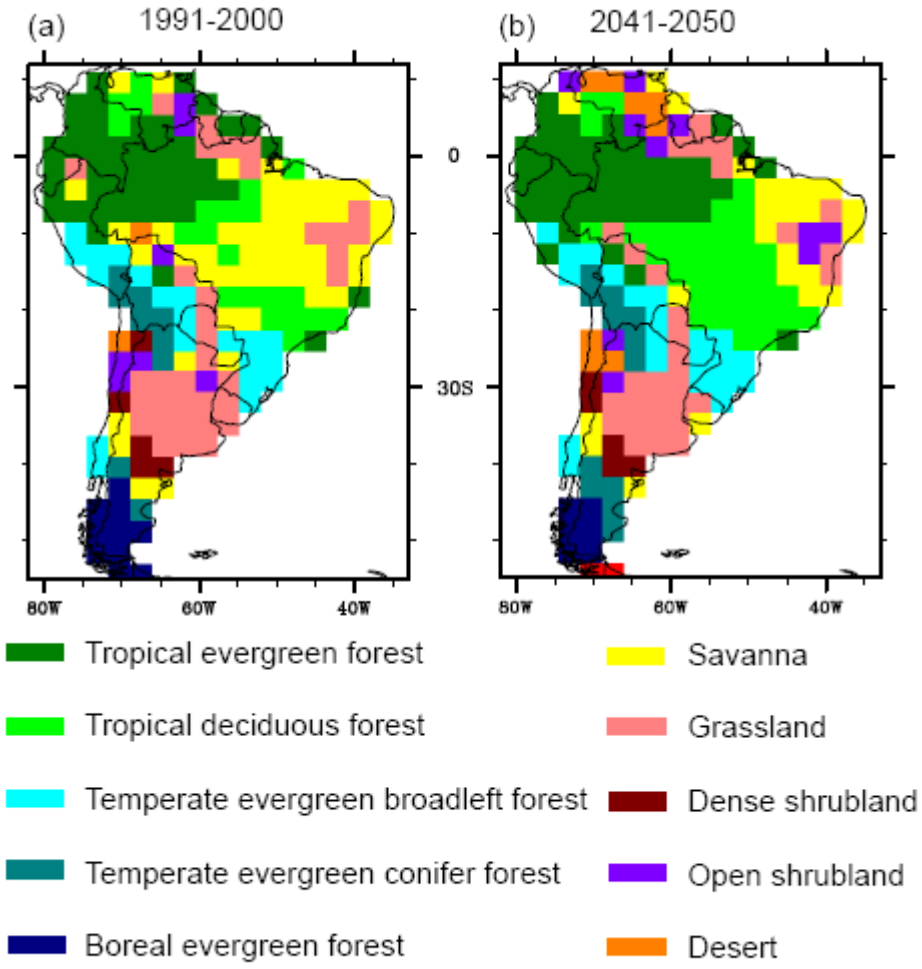

Figure 4 – Vegetation cover in South America, over present-day conditions (1991-2000) (a) and future scenario (2041-2050) (b).

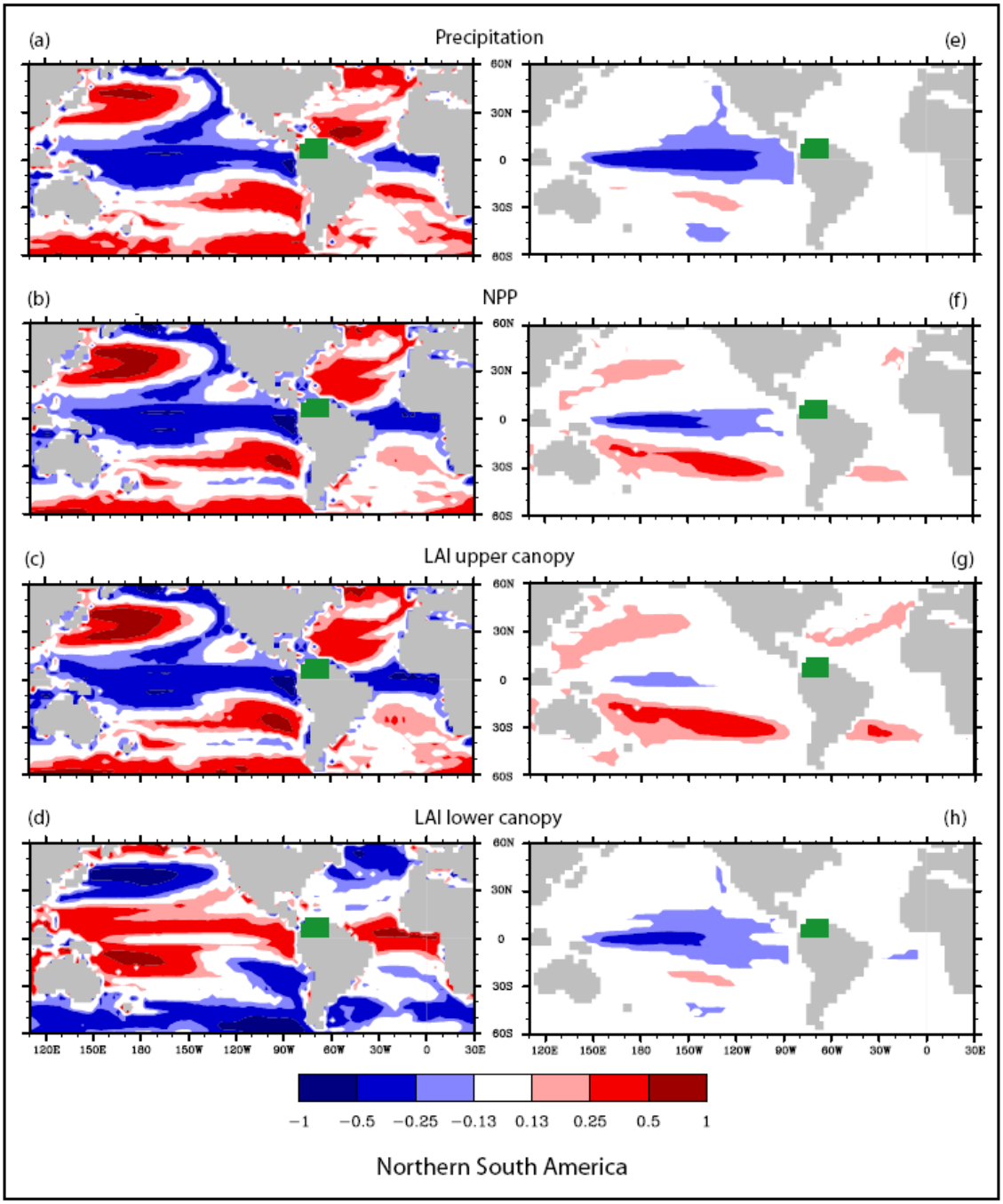

Figure 5 – Panels (a-h) illustrate the correlation between SST and climate, and vegetation patterns in NSA 2011-2050: where panels (a-d) are based on increased CO_2 atmospheric concentration for the A2 scenario of IPCC, and panels (e-h) illustrate the results without the trend of global warming (see text for details). It should be noted that these figures only show significant values at the 0.01 level with a positive or negative correlation of greater than 0.13.

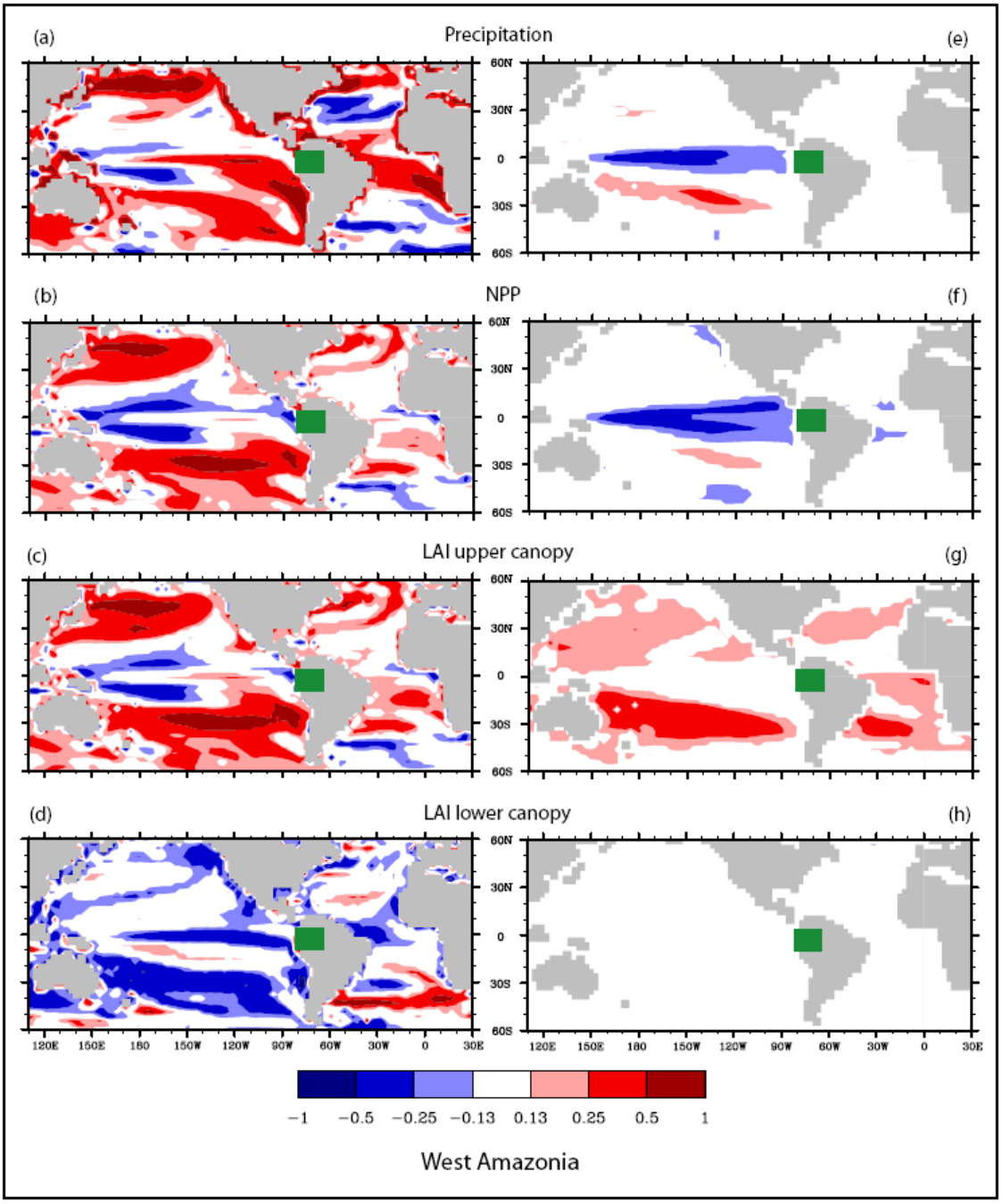

Figure 6 – Panels (a-h) illustrate the correlation between SST and climate, and vegetation patterns in WA 2011-2050: where panels (a-d) are based on increased CO_2 atmospheric concentration for the A2 scenario of IPCC, and panels (e-h) illustrate the results without the trend of global warming (see text for details). It should be noted that these figures only show significant values at the 0.01 level with a positive or negative correlation of greater than 0.13.

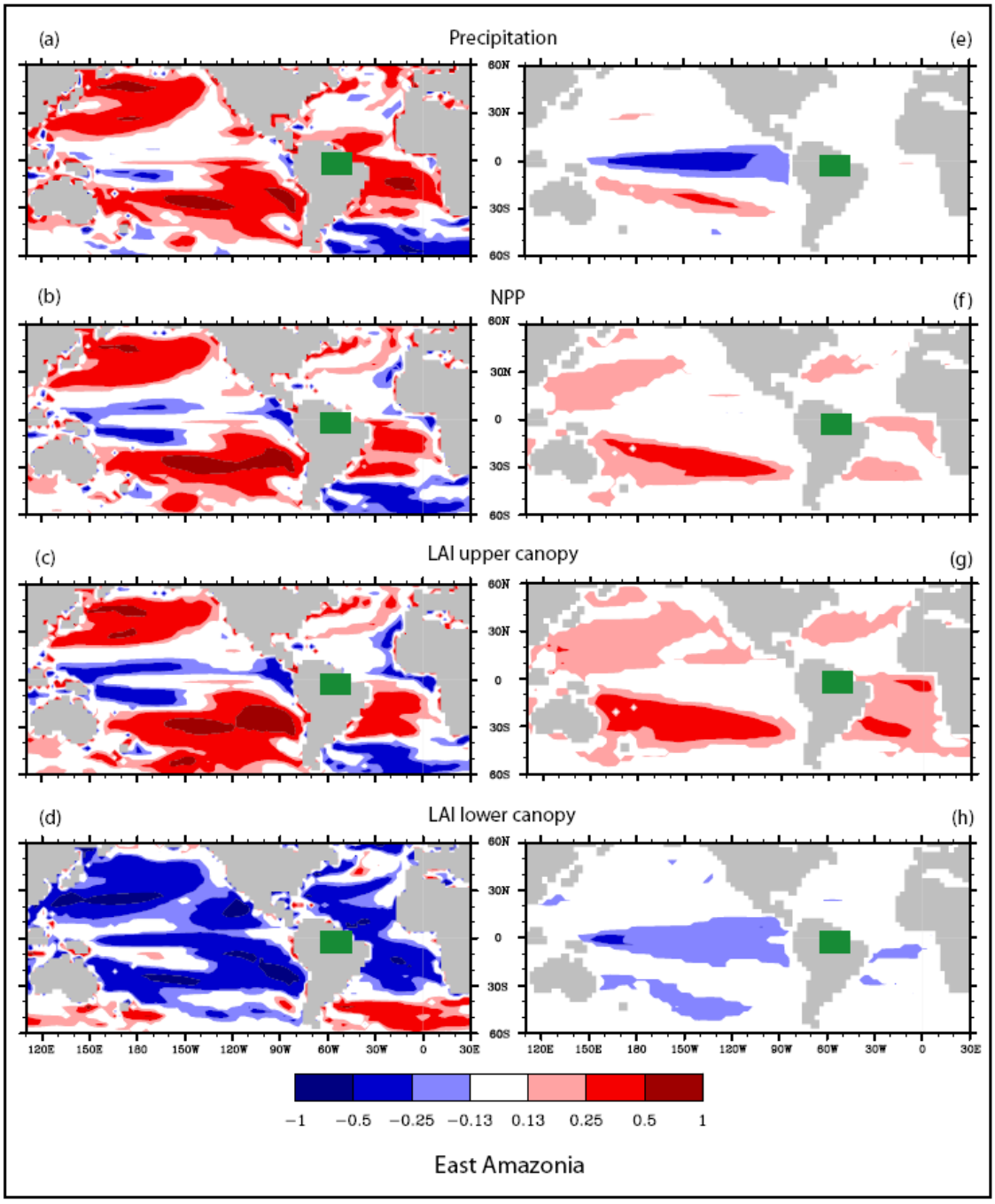

Figure 7 – Panels (a-h) illustrate the correlation between SST and climate, and vegetation patterns in EA 2011-2050: where panels (a-d) are based on increased CO_2 atmospheric concentration for the A2 scenario of IPCC, and panels (e-h) illustrate the results without the trend of global warming (see text for details). It should be noted that these figures only show significant values at the 0.01 level with a positive or negative correlation of greater than 0.13.

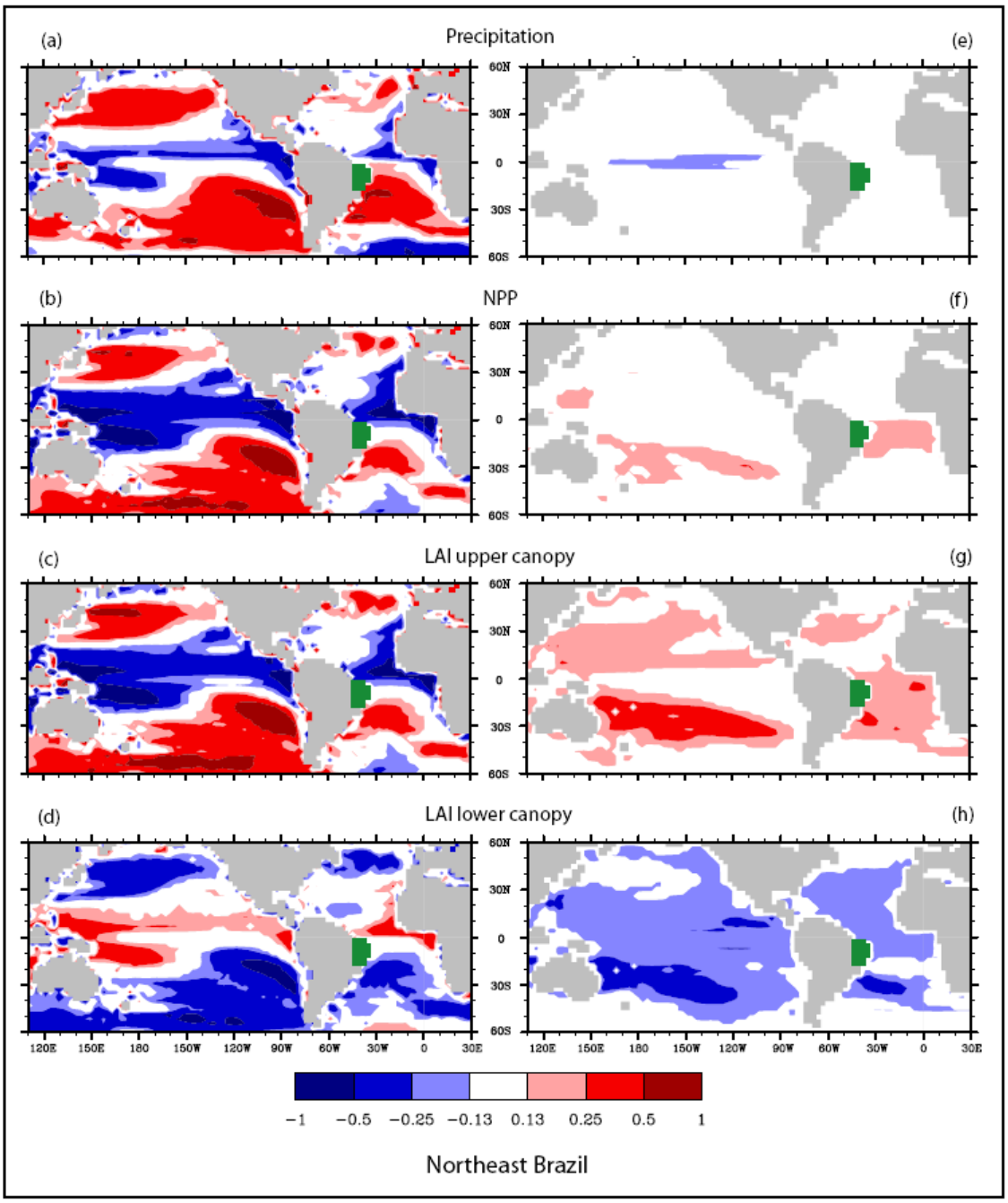

Figure 8 – Panels (a-h) illustrate the correlation between SST and climate, and vegetation patterns in NEB 2011-2050: where panels (a-d) are based on increased CO_2 atmospheric concentration for the A2 scenario of IPCC, and panels (e-h) illustrate the results without the trend of global warming (see text for details). It should be noted that these figures only show significant values at the 0.01 level with a positive or negative correlation of greater than 0.13.

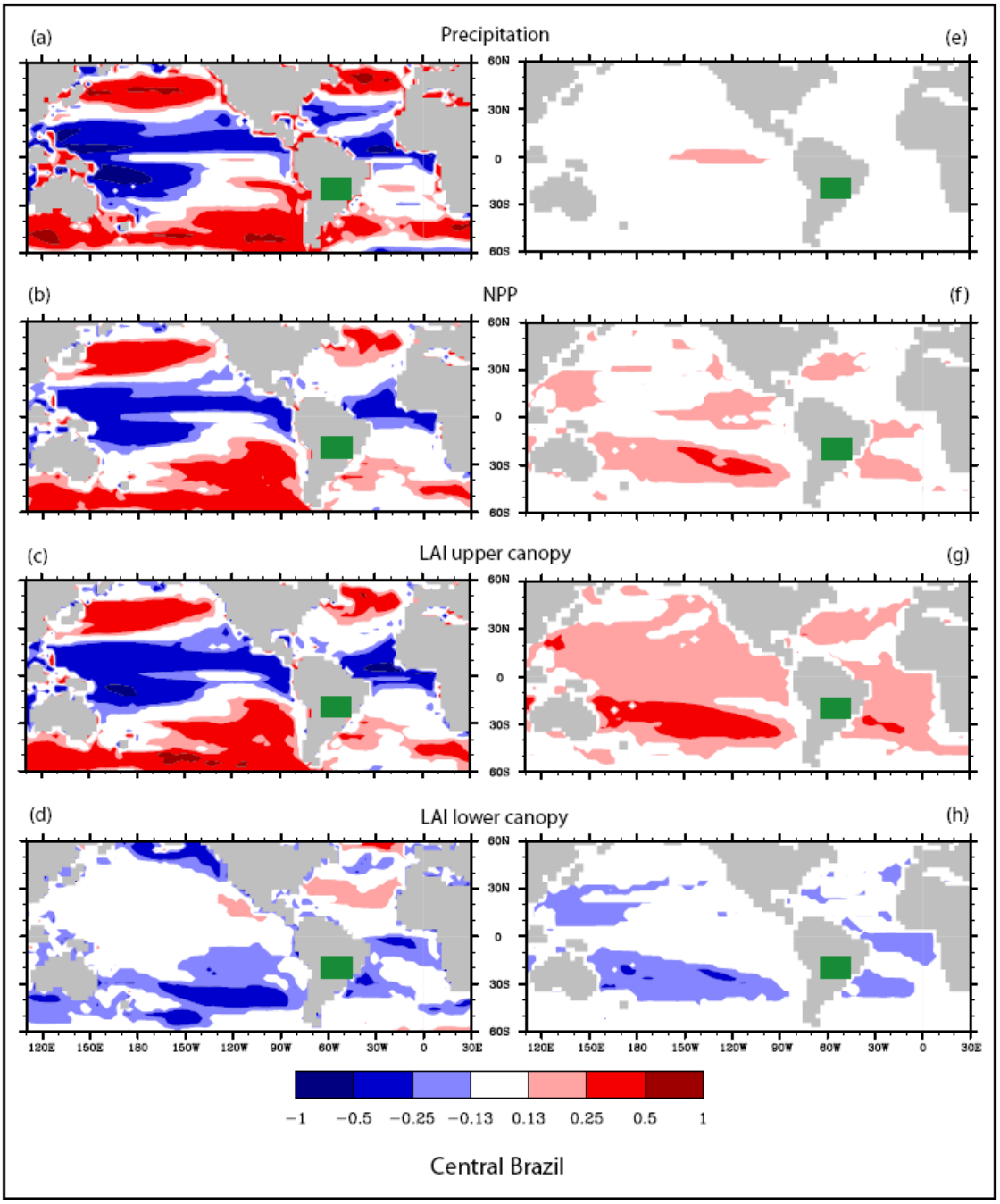

Figure 9 – Panels (a-h) illustrate the correlation between SST and climate, and vegetation patterns in CB 2011-2050: where panels (a-d) are based on increased CO_2 atmospheric concentration for the A2 scenario of IPCC, and panels (e-h) illustrate the results without the trend of global warming (see text for details). It should be noted that these figures only show significant values at the 0.01 level with a positive or negative correlation of greater than 0.13.

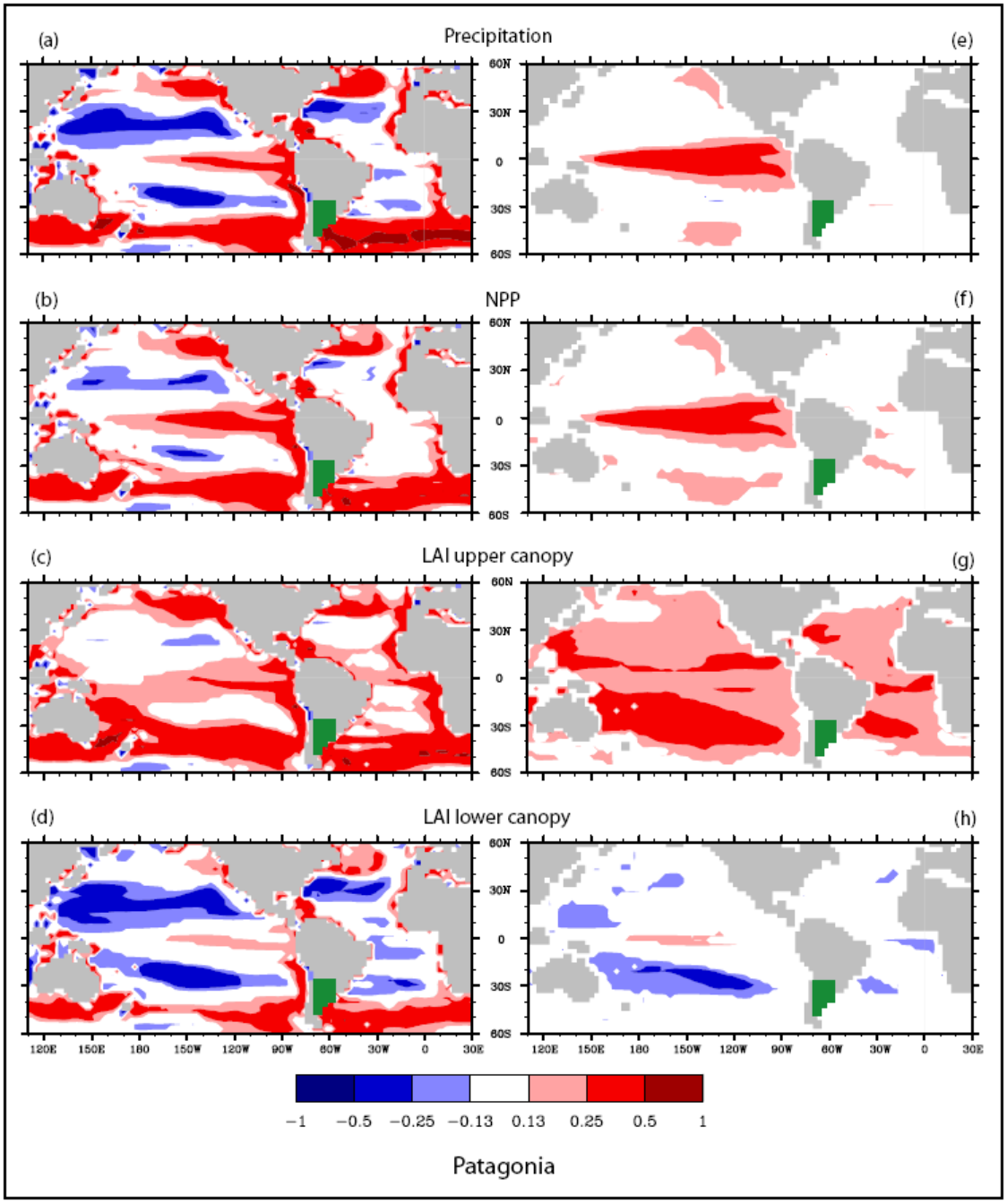

Figure 10 – Panels (a-h) illustrate the correlation between SST and climate, and vegetation patterns in PA 2011-2050: where panels (a-d) are based on increased CO_2 atmospheric concentration for the A2 scenario of IPCC, and panels (e-h) illustrate the results without the trend of global warming (see text for details). It should be noted that these figures only show significant values at the 0.01 level with a positive or negative correlation of greater than 0.13.

Capítulo 3

Pereira, M.P.S.; Costa, M.H.; and Machado, A.C.M. **Predicting land cover changes in the Amazon forest: an ocean-atmosphere-biosphere problem**. Manuscript to be submitted to Geophysical Research Letters.

Abstract

Accurate studies of the impacts of climate change on the distribution of major vegetation types are essential for developing effective conservation and land use policy. Such studies require the development of models that accurately represent the complex and interacting biophysical factors that influence regional patterns of vegetation. Here we investigate the impacts of Sea Surface Temperature (SST) on the vegetation of the Amazon, testing the hypothesis that changes in Amazonian vegetation structure are a consequence of an ocean-atmosphere-biosphere interaction. We design a numerical experiment in which we force a coupled climate-biosphere model by 10 SST patterns produced by different IPCC AR4 models, for the A2 scenario for the period 2001-2050. Simulations for 2011-2050 show that certain patterns of SST are likely to decrease the ensemble for tropical evergreen rainforest and savanna, and that these areas will be occupied mainly by tropical seasonal rainforest.

1. Introduction

One of the most important challenges in environmental science is to understand and predict the influence of climate change on the major ecosystems of the world. The focus of much of this research (reviewed by Malhi et al., 2008) has been the relatively pristine tropical forests of the Amazon basin in South America - the largest remaining area of continuous rainforest in the world and a vital component in maintaining global ecosystem services (*sensu* Constanza et al., 1998) such as hydrological cycles that have potential impacts on the regional and global climate system (Chahine, 1992; Cox et al., 2001; Werth and Avissar, 2002).

However, despite decades of empirical research and considerable advances in modeling there is still uncertainty regarding the fate of the Amazon under global warming. For example, it has been proposed that the Amazon forest may experience a dieback during

the 21th century as a consequence of anthropogenically induced global warming (Cox et al., 2000). Specifically, Cox and his colleagues predicted that forests of Amazonia would begin to be lost due to a drying and warming of the atmosphere based on the results of a fully coupled, three-dimensional carbon-climate model. Although they accept that this scenario rests upon "uncertain aspects of regional climate change, and may be 'short-circuited' by direct human deforestation" (p. 186). Huntingford et al. (2008) also predict die back based on the results of perturbed physics simulations covering a wide range of climate sensitivity. The effects of forest die back could, in turn, release more CO_2 into the atmosphere leading to further warming (Betts et al., 2004).

By contrast, some studies (e.g. Levis et al., 2000) have found that rising CO_2 would not significantly modify land cover in Amazonia. One of the key variables generating much of the uncertainty is precipitation, the prediction of which has remained problematic. As Malhi et al. (2009) point out; much of the discussion about the possibility of Amazon dieback has been based on either a single model, perturbed physics ensembles of a single model, or the uncritical examination of the results of a number of models. To remedy this situation Malhi et al. (2009) assessed the output of 19 IPCC AR4 Global Climate Models under the medium-high range A2 Emissions Scenarios. The results of the various models varied considerably (a few studies suggested an increase in precipitation in Amazonia during 21th century, others suggested a decrease, and the model mean was close to zero), although there was reasonable evidence to suggest that changes in the rainfall regime in East Amazonia may cause a transition to seasonal forest in this area (Malhi et al., 2009).

The huge variation in the forecasts for precipitation in the Amazon region under global warming strongly suggests that the models are failing to capture an important component of the hydrological cycle. A strong candidate for this missing factor is sea surface temperature (SST), patterns of which in the Pacific and Atlantic oceans are known to strongly influence the South American climate (Nobre and Shukla, 1996; Diaz et al., 1998; Grimm et al., 2000; Haylock et al., 2006). Although SST has been shown to strongly influence the predictions of coupled climate-vegetation models (Jiang et al., 2011), at a global scale, its potential influence on the future climate-vegetation coupled system in Amazonia has not been addressed.

Here we hypothesize that the vegetation in Amazonia in the 21th century will be a consequence of an ocean-atmosphere-biosphere interaction with the objective of producing more accurate regional forecasts of precipitation under global warming. To test this hypothesis, we design a numerical experiment in which we force a coupled climate-biosphere model by 10 SST patterns produced by different IPCC AR4 models, for the A2 scenario for

the period 2001-2050. We then analyze the results for the period 2011-2050 in order to demonstrate the relationship between land cover (tropical evergreen rainforest, tropical seasonal rainforest and savanna) and specific patterns of SST.

2. Model description and experiment design

In this work, we performed simulations using the CCM3 (Community Climate Model) general circulation model coupled to the surface model IBIS (Integrated Biosphere Simulator); a combination known as CCM3-IBIS and commonly used in simulation studies (e.g. Senna et al., 2009). Detailed information on the models is documented in Kiehl et al., (1998) and Foley et al., (1996), and will not be repeated here. The simulations were performed at T42 resolution (2.81° x 2.81°) and 18 levels in the vertical in the atmosphere and used a hybrid sigma-pressure coordinate system with a 15 minute time step interval. CCM3-IBIS incorporates the most recent dynamics scheme and parameterized physics for the Amazon rainforest region in order to reproduce bi-directional interactions between vegetation and climate (Foley et al., 2000; Senna et al., 2009) making it a useful tool for studying biome distribution, ecosystem functioning, and climate feedbacks in face of global climate change and land use change.

The performance of the CCM3-IBIS model in simulating the regional climate for the Amazon rainforest is described in detail by Senna et al. (2009). They reported that annual mean precipitation is within 10% of five datasets precipitation mean, and precipitation seasonality is also robustly simulated.

CCM3-IBIS was run for the period 1951-2050, to investigate the influence of variability in SST on vegetation cover in the Amazon forest through ten experimental simulations. SST data was obtained from PCMDI (Program for Climate Model Diagnosis and Inter-comparison). The 20th century period (1951-2000) was used to spin up the model. Ten representative outputs of the coupled climate models were chosen out of those used the 21th century SST under the A2 emission scenario by the IPCC in AR4 on the basis of spatial resolution and including a representative sample of meteorological research centers: CCCMA CGM3.1 T47, CNRM CM3, CSIRO MK3.0, GFDL CM2.1, GISS MODEL E_R, IPSL CM4, MIROC3.2 MEDRES, MPI ECHAM5, NCAR CCSM3.0 and UKMO HadCM3. More information about the models can be found at www-pcmdi.llnl.gov/ipcc. In addition to SST, all simulations were forced by atmospheric concentrations of CO_2 and CH_4 in accordance with the IPCC A2 scenario. Each simulation was spun up with dynamic vegetation and three repetitions (ensembles) per treatment, with runs starting on 17-19 January 2001, to obtain a

more realistic representation of vegetation and of climate situations for the same time period. The total experiment analyzed data included a total of 1650 years of simulation.

3. Results and Discussion

There is a clear pattern of change and replacement of major ecosystems in Amazonia in the first half of the 21th century in response to increased temperature and CO_2 (Figure 1). Specifically, the probability of decadal vegetation occurrence generated by CCM3-IBIS simulation ensembles reveals a clear temporal trend of decreasing tropical evergreen forest and savanna and increasing tropical deciduous forest (Figure 1). This result suggests that increases of deciduous forest are the main feature of the changes in vegetation composition under future global warming in the Amazon forest – this is in concordance with other regional modeling studies in the region (Malhi et al., 2009; Jing et al., 2011). The rate of transition increases in the second half of the study period as do the uncertainties (represented by the internal variability amplitudes). The increase in uncertainty is associated with the natural variability of internal processes within the climate system in the model and variability in the ten future patterns of SST (Figure 1).

Present-day climate conditions in Amazonia favor the occupation of the dominant tropical evergreen forest in almost 60% of the study area (11°N to 12°S by 49°W to 80°W), while savanna takes up approximately 35% and tropical deciduous forest occupies less than 5%. Global warming is predicted to affect vegetation in the next 40 years by reducing the cover of tropical evergreen forest by around 10% (approximately 50% of the total land cover) and savanna by around 5% (approximately 30% of the total land cover). Salazar et al. (2007) estimated a 9% reduction in Amazon forest cover during the period 2050–2059 – a value similar to that reported here. However, Salazar's study predicted replacements of forest by savanna vegetation while the present study supports the hypothesis that increasing CO_2 will stimulate the growth of tropical deciduous forest which is predicted to occupy the space lost by the other two vegetation types: Deciduous forest is predicted to occupy approximately 15% of the total Amazonian land cover by 2050 (Figure 1). Regions of transitional vegetation between savanna and tropical evergreen forest are predicted to become tropical deciduous forest.

We then select the ensembles with the highest (top 10%) levels of tropical evergreen rainforest, tropical seasonal rainforest and savanna and calculate the mean SST pattern associated with them (Figure 2a-c) and the difference among them (Figure 2d-f). This analysis suggests that specific patterns of SST can be identified that favor (through their influence on

Amazonian precipitation) each of the three ecosystems. Thus, a pattern of SST of below 29°C reaching temperatures of 23°C in the Equatorial Pacific (i.e. characteristic of a La Nina event) produces precipitation patterns that promote tropical evergreen forest coverage (Figure 2a).

Tropical deciduous forest is favored when there are SST conditions of around 29°C in the Equatorial Pacific and SST above 28°C across the tropical North Atlantic region (i.e. characteristic of the Atlantic Multidecadal Oscillation, AMO positive phase) (Figure 2b). Savanna is associated with SST patterns in Equatorial Pacific with regions of around 29°C (i.e. characteristic of the El Nino event), and across Tropical Atlantic regions with SST above 27°C (Figure 2c). The difference between SST patterns for the tropical seasonal rainforest and tropical evergreen rainforest shows positive anomalies in the North Atlantic and North Pacific Equatorial Oceans, and negative anomalies in the South Pacific (Figure 2d). The difference between SST patterns associated with savanna and tropical evergreen rainforest ensembles shows positive anomalies in the Equatorial Pacific region and negative anomalies in the South Atlantic and South Pacific equatorial Oceans (Figure 2e). Furthermore, SST difference patterns between savanna and tropical seasonal rainforest produce positive anomalies in the Equatorial Pacific, and negative anomalies in the North Atlantic and North Pacific Equatorial Oceans and the South Atlantic and South Pacific Equatorial Oceans (Figure 2f).

The relationship between SST and transitional vegetation in the Amazon forest under global warming scenarios can be best addressed through a statistical analysis of the patterns of variability. This spatial variation in SST is based on a series of bi-dimensional correlations between 10 future patterns of SST and Amazonian vegetation types (tropical evergreen rainforest, tropical seasonal rainforest and savanna) estimated from different SST scenarios for 2011-2050. These data are analyzed for 1200 years (3 ensembles x 10 SST patterns x 40 years) (Figure 3).

It has been well documented that anomalous warming or cooling of SST over the surrounding Pacific and Atlantic basins plays an important role in changes in precipitation in the Amazon region (e.g., Ronchail et al., 2002; Marengo, 1992; Yoon and Zeng, 2010). For example, an anomalously southward migration of the ITCZ during May–June 2009, due to the warmer than normal surface waters in the tropical South Atlantic, was responsible for abundant rainfall in large regions of eastern Amazonia from May to July 2009 (Marengo et al., 2011). The model demonstrates that tropical South Atlantic SSTs are positively correlated with rainfall in tropical evergreen rainforest and tropical deciduous (Figure 3a-b), and are negatively correlated with precipitation in the savanna region (Figure 3c). This means that the development of tropical evergreen rainforest and tropical deciduous rainforest over the

Amazon region is associated with anomalously warm SSTs in the tropical South Atlantic, and that the development of the savanna is associated with anomalously cold SSTs.

A warming of the tropical Atlantic in the north relative to the south leads to a northwestwards shift in the ITCZ and compensating atmospheric descent over Amazonia. Tropical North Atlantic SSTs exert a large influence on dry season rainfall in western Amazonia. For example, the Amazonian drought in 2005 was associated the persistent warm anomaly in the tropical North Atlantic that caused a delay onset of the South American monsoon (Cox et al., 2008). Our analysis of the probabilities of annual occurrence of Amazonian vegetation types shows that North Atlantic SSTs are negatively correlated with tropical evergreen rainforest and savanna (Figure 3a,c), and positive correlated with tropical deciduous forest (Figure 3b).

Simulations for the 21th century show a strong tendency for the SST conditions associated with the 2005 drought to become much more common. In other words, the North Atlantic region will warm more rapidly than the South Atlantic leading to a northwards movement of the ITCZ and suppression of July–October rainfall in western Amazonia (Cox et al., 2008). If this happens, climatic conditions will produce long dry seasons of the characteristics associated with the tropical deciduous rainforest environment. In the CCM3-IBIS model, drought resistant deciduous plants (including tropical deciduous trees, grasses) are assumed to respond to changes in the net canopy carbon budget. The mean (using a 10-day running average) net photosynthesis rate calculated by IBIS becomes negative (indicating that leaf respiration now exceeds gross photosynthesis) due to leaf loss (Kucharik et al., 2000).

In 2010, the drought over the Amazon Rainforest started in early austral summer during El Niño and subsequently intensified as a consequence of the warming of the tropical North Atlantic (Marengo et al., 2011). The warming of SST along the tropical North Atlantic and equatorial of the Pacific during the 2010 drought, as measured by rainfall deficit, affected an area 1.65 times larger than the 2005 drought. Moreover, the decline in greenness during the 2010 drought spanned an area that was four times greater and more severe than in 2005. Notably, 51% of all drought-stricken forests showed greenness declines in 2010 compared to only 14% in 2005. Overall, the widespread loss of photosynthetic capacity of Amazonian vegetation due to the 2010 drought may represent a significant perturbation to the global carbon cycle (Xu et al., 2011).

Previous studies have shown that rainfall patterns over the northern part of the Amazon change significantly depending on the phase of El Niño–Southern Oscillation

(ENSO) (Kousky et al., 1984; Ropelewski and Halpert, 1987). By extension, ENSO also an important plays role in the vegetation types in the Amazon rainforest. The probabilities of annual occurrence of tropical evergreen rainforest over the Amazon forest region are positively correlated with SST in the North Subtropical and Equatorial Pacific regions (proportional to the PDO and ENSO face) (Figure 3a). However, the probability of annual occurrences of the savanna and tropical seasonal forest are negatively correlated with SST anomalies in the Equatorial Pacific (Figure 3b,c).

4. Conclusions

Forecasting of vegetation cover under climate change scenarios at a regional scale is important for effective land use planning, adaptation and mitigation measures. The results of this study using the CCM3-IBIS coupled model clearly demonstrate the significant influence of SST on precipitation patterns and, therefore, the dynamics of Amazonian vegetation over time. Thus, the incorporation of the SST patterns in the coupled climate-vegetation models is clearly important for improving projections of future vegetation cover in this region.

The probabilities of occurrence of the vegetation types in the Amazon rainforest is linked to anomalous warming or cooling of SST over the surrounding ocean basins of the Pacific and Atlantic. SSTs are especially important in the tropics because the atmosphere is sensitive to the oceanic and continental surface conditions, which greatly influence the variability of the climate. Our quantification of the potential changes in vegetation under global warming in first half of 21th century predicts a suite of changes that favor an increase in tropical seasonal rainforest and a decrease in both tropical evergreen rainforest and savanna vegetation.

Acknowledgements

We thank Amazonas and Minas Gerais State Research Funding Agencies (FAPEAM, FAPEMIG) for financial support. We also thank Dr Richard J. Ladle for reviewing the English and commenting on the manuscript.

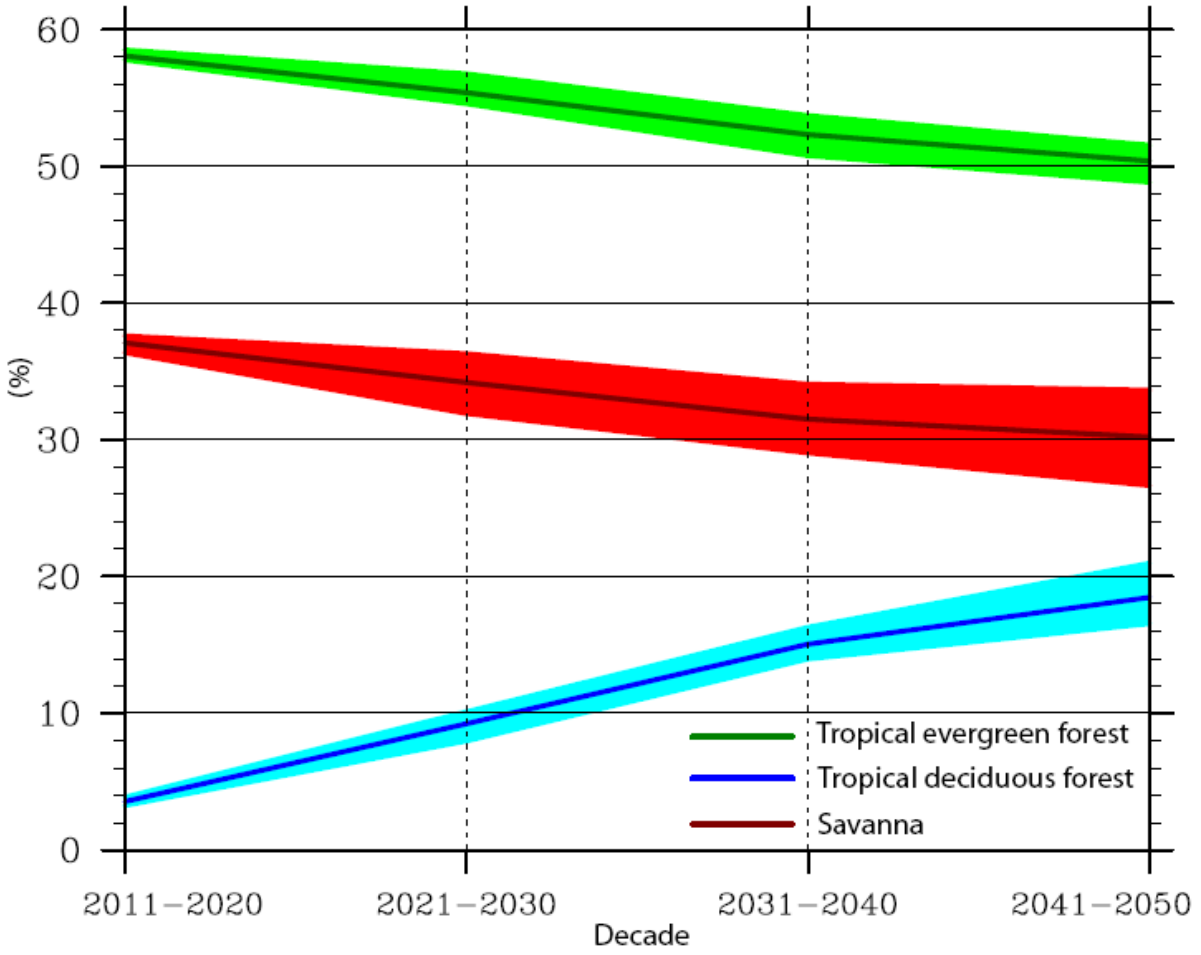

Figure 1. Probability of decadal vegetation occurrence in Amazonia (11°N to 12°S by 49°W to 80°W) as predicted by the CCM3-IBIS simulation ensembles (3 ensembles x 10 SSTs patterns x 10 years). Vegetation types = tropical evergreen forest (green), tropical deciduous forest (blue) and savanna (red). Shaded area indicates the uncertainty range (see text for explanation).

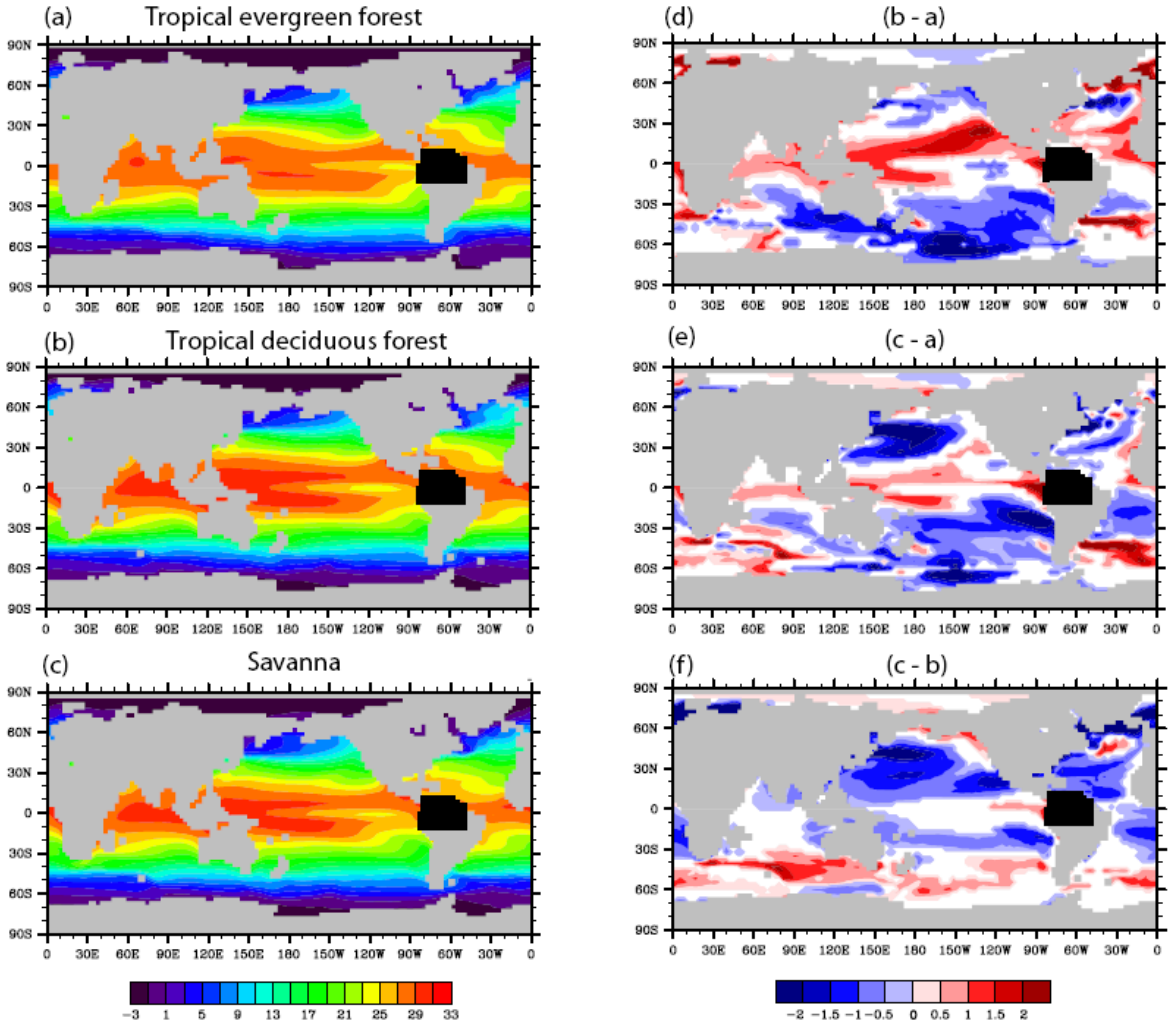

Figure 2. SST characteristics that produce climate conditions that favor certain vegetation types (tropical evergreen rainforest, tropical seasonal rainforest and savanna) in Amazon forest (2a-c), and the differences between them as labeled (2d-f). Only areas significant at the 95% level of a Student's t-test are illustrated.

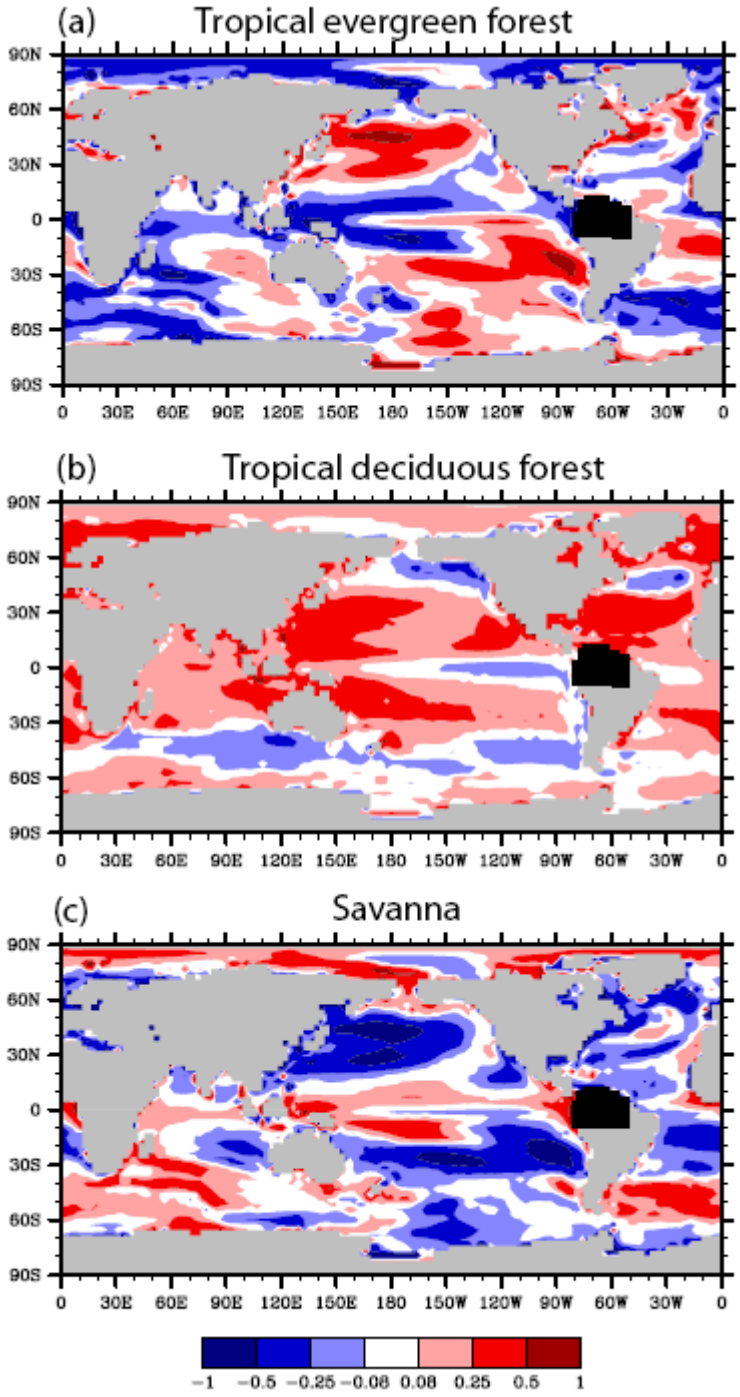

Figure 3. Spatial variation in SST based on a series of bi-dimensional correlations between 10 future patterns of SST and Amazonian vegetation types (tropical evergreen rainforest, tropical seasonal rainforest and savanna) estimated from different SST scenarios for 2011-2050 (3 ensembles x 10 SSTs patterns x 40 years). It should be noted that these figures only show significant values at the 0.01 level that show a positive or negative correlation of greater than 0.08.

Síntese

Com este trabalho pretendeu-se estudar as mudanças na estrutura da vegetação na América do Sul em função de diferentes cenários de clima para a primeira metade do século XXI, em particular considerando diferentes padrões de TSM. Objetivos principais eram os seguintes:

- Quantificar a incerteza nas previsões da vegetação para América do Sul causada por diferentes padrões de TSM.
- Avaliar a influência da variabilidade espaço-temporal da TSM sobre a dinâmica da vegetação na América do Sul.
- Por fim, investigar os impactos da TSM sobre a vegetação na Amazônia.

A presente tese enquadra-se na climatologia da América do Sul, a qual tem como objetivo principal a analise da variabilidade futura dos padrões de TSM e a procura das suas causas potenciais na vegetação. A climatologia privilegia a escala espacial regional e as escalas temporais sazonais, anuais e decadais. O passo de tempo normalmente utilizado é médias anuais. Nesta escala temporal uma fonte importante da variabilidade vem das interações do sistema oceano-atmosfera-biosfera, pois os processos físicos são mais lentos na variabilidade da TSM e vegetação, sendo mais evidentes na escala decadal.

O ponto fulcral deste trabalho foi a previsão dos padrões de vegetação em relação às mudanças climáticas na escala regional em resposta do aumento esperado do CO_2, privilegiando, sobretudo, as incertezas da projeção do modelo climático na cobertura da vegetação, e a correlação entre os padrões de TSM e as variáveis dos ecossistemas. Contudo, a validação do modelo CCM3-IBIS não foi esquecida, mas teve um menor grau de aprofundamento. Neste contexto, a análise dos dados de TSM no comportamento de vários ecossistemas na América do Sul, com ênfase maior na Amazônia, é a principal meta do trabalho.

A TSM foi o parâmetro central deste estudo e para a explicação da sua interação na América do Sul foram ainda utilizados parâmetros da atmosfera (precipitação) e de estrutura e dinâmica da vegetação (NPP, LAI e PFTs), a fim de diagnosticar impactos climáticos que influenciam o estado da vegetação sobre a região. Para verificar a capacidade do modelo CCM3-IBIS em reproduzir o clima durante o período em estudo na América do Sul, a

sazonalidade da precipitação da simulação de controle foi comparada com seis diferentes bancos de dados climáticos. A análise da variabilidade sazonal da precipitação foi feita em vários ecossistemas na América do Sul, regiões de diferentes características climáticas. Os resultados da precipitação simulada pelo CCM3-IBIS mostraram que estão de acordo com os seis bancos de dados climáticos. Uma descrição detalhada do modelo IBIS é mostrada no Apêndice A.

O diferencial deste trabalho é o uso do modelo totalmente acoplado biosfera-atmosfera (CCM3-IBIS) sendo forçado por padrões de TSM e gases de efeito estufa, com intuito de aprimorar o conhecimento da relação clima-vegetação na América do Sul. Para estudar este assunto, esta tese foi dividida em três capítulos, e a conclusão de cada capítulo é resumida abaixo.

O capítulo 1 demonstra como as diferentes previsões da TSM até 2050 aumentam a incerteza associada com as previsões da distribuição dos principais ecossistemas da América do Sul. A precisão exata de padrões de vegetação sob as mudanças climáticas em escala regional ou global em resposta ao aumento esperado do CO_2 é um pré-requisito vital para o planejamento efetivo do uso do solo, medidas de adaptação e mitigação. No entanto, tais simulações complexas, inevitavelmente, geram grandes incertezas, especialmente onde pequenas mudanças no clima podem levar a grandes transições no ecossistema. As simulações indicam que não é possível prever com robustez uma cobertura vegetal de uma área equivalente a 28% da América do Sul (5×10^6 km²), e os resultados nas regiões central e nordeste do Brasil é especialmente incerto, com a vegetação variando de savana, e pastagem para caatinga. Esse estudo é pioneiro em destacar e estimar algumas das incertezas associadas a esse processo de previsão ambiental na América do Sul.

O capítulo 2 investiga as correlações entre a variabilidade da TSM e vegetação em diferentes regiões da América do Sul. Os resultados demonstram claramente a influência significativa que a TSM pode desempenhar na dinâmica dos ecossistemas terrestre. Este estudo prevê que o aumento das emissões de CO_2 na atmosfera será acompanhado por mudança na precipitação, e com grande possibilidade das condições climáticas causarem mudanças notáveis na composição e estrutura da vegetação regional. No cerrado brasileiro a vegetação sofrerá mudanças visíveis, ficará mais densa através do aumento do LAI da parte superior do dossel, tornando-se uma floresta decídua. A conclusão geral deste capitulo, mostra que uma mudança na TSM é um fator importante na transformação/conservação da estrutura da vegetação da América do Sul.

O capítulo 3 investiga os impactos da TSM sobre a vegetação na Amazônia, testando a hipótese de que as mudanças na estrutura da vegetação na Amazônia são uma consequência de uma interação oceano-atmosfera-biosfera. Os resultados mostram que as probabilidades de ocorrência dos tipos de vegetação na floresta Amazônica estão relacionadas aos padrões de TSM sobre as bacias oceânicas do Pacifico e Atlântico. As simulações mostram que certos padrões de TSM para 2011-2050 podem ocasionar a diminuição das áreas de floresta tropical e savana, e que essas áreas serão ocupadas principalmente por floresta decídua.

O efeito das mudanças climáticas futuras na América do Sul, tais como incêndios florestais, tempestades, secas severas e aumento/diminuição na produtividade da vegetação, comandarão a atenção do público e aumentará a procura de recurso de gestão. O aumento da utilização dos modelos sofisticados e de parametrização adequadas (dinâmica clima-vegetação, TSM controlado) fornecerá uma previsão mais realista da vegetação sob as mudanças climáticas. Os resultados aqui apresentados indicam fortemente a necessidade de uma investigação mais aprofundada sobre o papel dos padrões de TSM na vegetação (e ecossistema terrestre em geral). Pesquisas futuras devem se concentrar em elucidar a natureza no complexo de interação oceano-atmosfera-biosfera, se há impactos sobre a distribuição da vegetação e na variabilidade climática. Outras exigências de estudos futuros é o desenvolvimento de novas ferramentas matemáticas e estatísticas, que permita não apenas estimar o impacto do clima futuro, mas também uma melhor quantificação das incertezas envolvidas nos experimentos climáticos.

Referências Bibliográficas

Aceituno, P.; Prieto, M. R.; Solari, M. E.; Martinez, A.; Poveda, G.; Falvey, M. 2009. The 1877-1878 El Niño episode: associated impacts in South America. *Clim. Change*, 92:389-416. DOI: 10.1007/s10584-008-9470-5.

Alo, C. A.; Wang, G. 2008. Potential future changes of the terrestrial ecosystem based on climate projections by eight general circulation models. *J Geophys Res*. 113:G01004. DOI: 10.1029/2007JG000528.

Andreoli, R. V.; Kayano, M. T. 2005. ENSO-related rainfall anomalies in South América and associated circulation features during warm and cold Pacific decadal oscillation regimes. *International Journal of Climatology*. 25:15:2017-2030.

Barsugli, J. J.; Shin, S. I.; Sardeshmukh, P. D. 2006. Sensitivity of global warming to the pattern of tropical ocean warming. *Clim Dyn*. 27:483-492.

Betts, R. A.; Cox, P. M.; Collins, M.; Harris, P. P.; Huntingford, C.; Jones, C. D. 2004. The role of ecosystem-atmosphere interactions in simulated Amazonian precipitation decrease and forest dieback under global climate warming. *Theor and Appl Climatol*. 78:157-175.

Betts, R. A.; Cox, P. M.; Lee, S. E.; Woodward, F. I. 1997. Contrasting physiological and structural vegetation feedbacks in climate change simulations. *Nature*. 387:796-799.

Botta, A.; Viovy, N.; Ciais, P.; Friedlingstein, P.; Monfray, P. 2000. A global prognostic scheme of leaf onset using satellite data. *Global Change Biology*, 6: 709-725.

Chahine, M. T. 1992. The hydrological cycle and its influence on climate. *Nature*. 359:373–380.

Cook, K. H.; Vizy, E. K. 2008. Effects of twenty-first-century climate change on the Amazon rain forest. *J Clim*. 21:542-560.

Cox, P. M.; Betts, R. A.; Collins, M.; Harris, P. P.; Huntingford, C.; Jones, C. D. 2004. Amazonian forest dieback under climate-carbon cycle projections for the 21st century. *Theor Appl Climatol*. 78:137-156.

Cox, P. M.; Betts, R. A.; Jones, C. D.; Spall, S. A.; Totterdell, I. J. 2000. Acceleration of global warming due to carbon-cycle feedbacks in a coupled climate model. *Nature* 408:184-187.

Cox, P. M.; Betts, *R. A*; Jones, C. D.; Spall, S. A.; Totterdell, *I. J.* 2001. Modelling vegetation and the carbon cycle as interactive elements of the climate system. *In: Meteorology at the millennium, (ed.* R.Pearce*), Academic Press, New York,* 14:795-825.

Cox, P. M.; Harris, P. P.; Huntingford, C.; Betts, R. A.; Collins, M.; Jones, C. D.; Jupp, T. E.; Marengo, J. A.; Nobre C. A. 2008. Increasing risk of Amazonian drought due to decreasing aerosol pollution. *Nature.* 453:8. DOI: 10.1038/nature06960.

Curtis, P. S. 1996. A meta-analysis of leaf gas exchange and nitrogen in trees grown under elevated carbon dioxide. *Plant, Cell and Environment,* 19:127-137.

Delire, C.; Levis, S. L.; Bonan, G.; Foley, J. A.; Coe, M.T.; Vavrus, S. 2002. Comparison of the climate simulated by the CCM3 coupled to two different land-surface models. *Clim Dyn.* 19:657–669.

Diaz, A. F.; Studzinski, C. D.; Mechoso, C. R. 1998. Relationships between precipitation anomalies in Uruguay and Southern Brazil and sea surface temperature in the Pacific and Atlantic Oceans. J Clim 11(2):251-271.

Farquhar, G. D.; Caemmerer, S. V.; Berry, J. A. 1980. A biogeochemical model of photosynthetic CO_2 assimilation in leaves of C3 species. *Planta*, 149: 78-90.

Field, C. B.; Jackson, R. B.; Mooney, H. A. 1995. Stomatal responses to increased CO_2: Implications from the plant to the global scale. *Plan, Cell Environ*. 18:1214-1225.

Foley, J. A.; Prentice, I. C.; Ramankutty, N.; Levis, S.; Pollard, D.; Sitch, S.; Haxeltine, A. 1996. An integrated biosphere model of land surface processes, terrestrial carbon balance, and vegetation dynamics. *Global Biogeochem Cycles*. 10:603-628.

Foley, J. A.; Levis, S.; Costa, M. H.; Cramer, W.; Pollard, D. 2000. Incorporating dynamic vegetation cover within global climate models. *Ecol. Appl.* 10(6):1620-1632. DOI:10.1890/1051-0761(2000)010[1620:IDVCWG]2.0.CO;2.

Fu, R.; Dickinson, R. E.; Chen, M.; Wang, H. 2001. How do tropical sea surface temperatures influence the seasonal distribution of precipitation in the equatorial Amazon? *J Clim.* 14(20):4003-4026.

Grimm, A. M.; Barros, V. R.; Doyle, M. E. 2000. Climate variability in Southern South América associated with El Niño and La Niña events. *J Clim.* 13:35-58.

Grimm, A. M. 2003. The El Niño Impact on the Summer Monsoon in Brazil: Regional Processes versus Remote Influences. *J. Clim.* 16:263–280.

Haylock, M. R.; Peterson, T. C.; Alves, L. M.; Ambrizzi, T.; Anunciação, Y. M. T; Baez, J.; Barros, V. R.; Berlato, M. A.; Bidegain, M.; Coronel, G.; Corradi, V.; Garcia, V. J.; Grimm, A. M.; Karoly, D.; Marengo, J. A.; Marino, M. B.; Moncunill, D. F.; Nechet, D.;

Quintana, J.; Rebello, E.; Rusticucci, M.; Santos, J. L.; Trebejo, I.; Vincent, L. A. 2006. Trends in total and extreme South Américan rainfall in 1960-2000 and links with sea surface temperature. *J Clim.* 19:1490-1512.

Hawkins, E.; Sutton, R. 2009. The potential to narrow uncertainty in regional climate predictions. *Bull. Am. Meteorol. Soc.* 90:1095. DOI:10.1175/2009BAMS2607.1

Hegerl, G. C.; Zwiers, F. W.; Braconnot, P.; Gillett, N. P.; Luo, Y.; Marengo, J. A.; Nicholls, N.; Penner, J. E.; Stott P. A. 2007. Understanding and attributing climate change, In: Solomon, S.; Qin, D.; Manning, M.; Chen, Z.; Marquis, M.; Averyt, K. B.; Tignor, M.; Miller H. L. (eds) Climate change 2007: the physical science basis. Contribution of Working Group I to the fourth assessment report of the intergovernmental panel on climate change. Cambridge University Press. *Cambridge and New York.* pp 663–745.

Huffman, G. J.; Adler, R. F.; Arkin, P.; Chang, A.; Ferraro, R.; Gruber, A.; Janowiak, J.; McNab, A.; Rudolf, B.; Schneider, U. 1997. The Global Precipitation Climatology Project (GPCP) combined precipitation dataset. *Bull. Am. Meteorol. Soc.* 78:5–20.

Huntingford, C.; Fisher, R. A; Mercado, L.; Booth, B. B. B.; Sitch, S.; Harris, P. P.; Cox, P. M.; Jones, C. D.; Betts, R. A.; Malhi, Y.; Harris, G. R.; Collins, M.; Moorcroft, P. 2008. Towards quantifying uncertainty in predictions of Amazon "dieback". *Philos. Trans. R. Soc.*, Ser. B. 363(1498):1857–1864. DOI:10.1098/rstb.2007.0028.

Jiang, D.; Zhang, Y.; Lang, X. 2011. Vegetation feedback under future global warming. *Theor. Appl. Climatol.* DOI:10.1007/s00704-011-0428-6.

Kalnay, E.; Kanamitsu, M.; Kistler, R.; Collins, W.; Deaven, D.; Gandin, L.; Iredell, M.; Saha, S.; White, G.; Woollen, J.; Zhu, Y.; Leetmaa, A.; Reynolds, R.; Chelliah, M.; Ebisuzaki, W.; Higgins, W.; Janowiak, J.; Mo, K. C.; Ropelewski, C.; Wang, J.; Jenne, R. Joseph, D. 1996. The NCEP/NCAR 40-Year Reanalysis Project. *Bull. Am. Meteorol. Soc.* 77:437–471.

Kiehl, J. T.; Hack, J. J.; Bonan, G. B.; Boville, B. A.; Williamson, D. L.; Rasch, P. J. 1998. The National Center for Atmospheric Research Community Climate Model: CCM3. *J. Climate.* 11(6):1131-1149.

Kousky, V. E.; Kayano, M. T.; Cavalcanti, I. F. A. 1984. A review of the Southern Oscillation: oceanic-atmospheric circulation changes and related rainfall anomalies. *Tellus A.* 36A:490–504. DOI:10.1111/j.1600-0870.1984.tb00264.x.

Kucharik, C. J.; Foley, J. A.; Delire, C.; Fisher, V. A.; Coe, M. T.; Lenters, J. D.; Young-Molling, C.; Ramankutty, N. 2000. Testing the performance of a dynamic global

ecosystem model: water balance, carbon balance, and vegetation structure. *Global Biogeochem Cycles*. 14:795-825.

Lapola, D. M.; Oyama, M. D; Nobre, C. A. 2009. Exploring the range of climate biome projections for tropical South America: The role of CO_2 fertilization and seasonality, Global Biogeochem. Cycles, 23, GB3003, doi:10.1029/2008GB003357.

Levis, S.; Foley, J. A.; Pollard, D. 2000. Large scale vegetation feedbacks on a doubled CO_2 climate. *J. Climate.* 13(7):1313-1325. DOI:10.1175/1520-0442(2000)013<1313:LSVFOA>2.0.CO;2.

Malhi, Y.; Aragão, L. E. O. C.; Galbraith, D.; Huntingford, C.; Fisher, R.; Zelazowski, P.; Sitch, S.; McSweenney, C.; Meir, P. 2009. Exploring the likelihood and mechanism of a climate-change-induced dieback of the Amazon rainforest. *Proc Natl Acad Sci U S A*. 106(49):20610–20615. DOI:10.1073/pnas.0804619106.

Malhi, Y.; Roberts, J. T.; Betts, R. A.; Killeen, T. J.; Li, W.; Nobre, C. A. 2008. Climate Change, Deforestation, and the Fate of the Amazon. *Science.* 319:169–172, DOI:10.1126/science.1146961.

Marengo, J. 1992. Interannual variability of surface climate in the Amazon basin, *Int. J. Climatol.* 12:853–863.

Marengo J. A., C. A. Nobre, J. T., M. D. Oyama, G. S. de Oliveira, R. de Oliveira, H. Camargo, L. M. Alves, and I. F. Brown (2008), The Drought of Amazonia in 2005, *J. Clim.*, 21, 495-516, doi:10.1175/2007JCLI1600.1.

Marengo, J.A.; Tomasella, J.; Soares, W. R.; Alves, L. M.; Nobre, C. A. 2011. Extreme climatic events in the Amazon basin. *Theor. Appl. Climatol.* DOI:10.1007/s00704-011-0465-1.

Marengo, J. A.; Tomasella, J.; Alves, L. M.; Soares, W. R.; Rodriguez, D. A. 2011. The drought of 2010 in the context of historical droughts in the Amazon region. *Geophys. Res. Lett.* 38:L12703. DOI:10.1029/2011GL047436.

Mokhov, I. I.; Demchenko, P. F.; Eliseev, A. V.; Khon, V. Ch.; Khvorost'yanov, D. V. 2002. Estimation of global and regional climate changes during the 19th-21st centuries on the basis of the IAP RAS model with consideration for anthropogenic forcing. *Izvestiya, Atmospheric and Oceanic Physics*, 38. 5:555-568.

New, M.; Hume, M.; Jones, P. 1999. Representing twentieth century space-time climate variability: 1. Development of a 1961-1990 mean monthly terrestrial climatology. *J. Climate.* 12:829-856.

Nobre, P.; Shukla, J. 1996. Variations of sea surface temperature, wind stress, and rainfall over the Tropical Atlantic and South America. *J. Climate.* 9(10):2464-2479. DOI:10.1175/1520-0442(1996)009<2464:VOSSTW>2.0.CO;2.

O'ishi, R.; Abe-Ouchi, A. 2009. Influence of dynamic vegetation on climate change arising from increasing CO_2. *Clim. Dynam.* 33:645–663. DOI:10.1007/s00382-009-0611-y.

Polley, H. W.; Johnson, H. B.; Marino, B. D.; Mayeux, H. S. 1993. Increase in C3 plant water-use efficiency and biomass over Glacial to present CO_2 concentrations. *Nature.* 361:61-64.

Rammig, A.; Jupp, T.; Thonicke, K.; Britta, T.; Heinke, J.; Ostberg, S.; Lucht, W.; Cramer, W.; Cox, P. 2010. Estimating the risk of Amazonian forest dieback. *New Phytol.* DOI:10.1111/j.1469-8137.2010.03318.x

Ronchail, J.; Cochonneau, G.; Molinier, M.; Guyot, J-L.; Chaves, A. G. M.; Guimarães, V.; Oliveira, E. 2002. Interannual rainfall variability in the Amazon basin and sea-surface temperatures in the equatorial Pacific and the tropical Atlantic oceans. *Int. J. Climatol.* 22:1663–1686. *DOI*:10.1002/joc.815.

Ropelewski, C. F.; Halpert, M. S. 1987. Global and regional scale precipitation patterns associated with the El Niño/Southern Oscillation. *Mon. Weather Rev.* 115:1606–1626.

Salazar, L. F.; Nobre, C. A.; Oyama, M. D. 2007. Climate change consequences on the biome distribution in tropical South America. *Geophys. Res. Lett*. 34:L09708.

Sellers, P. J.; Bounoua, L.; Collatz, G. J.; Randall, D. A.; Dazlich, D. A.; Los, S. O.; Berry, J. A.; Fung, I.; Tucker, C. J.; Field, C. B.; Jensen, T. G. 1996. Comparison of radiative and physiological effects of doubled atmospheric CO_2 on climate. *Science*. 271(5254):1402-1406.

Senna, M. C. A.; Costa, M. H.; Pinto, L. I. C.; Imbuzeiro, H. M. A.; Diniz, L. M. F.; Pires, G. F.; 2009. Challenges to reproduce vegetation structure and dynamics in Amazonia using a coupled climate-biosphere model. *Earth Interact.* DOI:10.1175/2009EI281.1.

Tebaldi, C.; Knutti, R. 2007. The use of the multimodel ensemble in probabilistic climate projections. *Phil. Trans. R. Soc. A.* 365:2053–2075.

Thomas, C. D.; Cameron, A.; Green, R. E.; Bakkenes, M. ; Beaumont, L.J.; Collingham, Y. C.; Erasmus, B. F. N.; Ferreira de Siqueira, M.; Grainger, A.; Hannah, L.; Hughes, L.; Huntley, B.; van Jaarsveld, A. S.; Midgley, G. F.; Miles, L.; Ortega-Huerta, M. A.; Peterson, A. T.; Phillips, O. L.; Williams, S. E. 2004. Extinction risk from climate change. *Nature*. 427:145-148. doi:10.1038/nature02121.

Trenberth, K. E.; Jones, P. D.; Ambenje, P.; Bojariu, R.; Easterling, D.; Klein Tank, A.; Parker, D.; Rahimzadeh, F.; Renwick, J. A.; Rusticucci, M.; Soden, B.; Zhai, P. 2007. Observations: surface and atmospheric climate change, In: Solomon, S.; Qin, D.; Manning, M.; Chen, Z.; Marquis, M.; Averyt, K. B.; Tignor, M.; Miller, H. L. (eds) Climate Change 2007: the physical science basis, contribution of Working Group I to the fourth assessment report of the intergovernmental panel on climate change, Cambridge University Press. *Cambridge and New York*. 235–336.

Uppala M.; Kallberg, P. W.; Simmons, A. J.; Andrae, U.; Da Costa Bechtold, V.; Fiorino, M.; Gibson, J. K.; Haseler, J.; Hernandez, A.; Kelly, G. A.; Li, X.; Onogi, K.; Saarinen, S.; Sokka, N.; Allan, R. P.; Andersson, E.; Arpe, K.; Balmaseda, M. A.; Beljaars, A. C. M.; Vande Berg, L.; Bidlot, J.; Bormann, N.; Caires, S.; Chevallier, F.; Dethof, A.; Dragosavac, M.; Fisher, M.; Fuentes, M.; Hagemann, S.; Ho´ Lm, E.; Hoskins, B. J.; Isaksen, L.; Janssen, P. A. E. M.; Jenne, R.; Mcnally, A. P.; Mahfouf, J.-F.; Morcrette, J.-J.; Rayner1, N. A.; Saunders, R. W.; Simon, P.; Sterl, A.; Trenberth, K. E.; Untch, A.; Vasiljevic, D.; Viterbo, P.; Woollen, J. 2005. The ERA-40 Re-Analysis. Q. J. R. *Meteorolog. Soc*. 131:2961–3012. DOI:10.1256/qj.04.176.

Werth, D.; Avissar, R. 2002. The local and global effects of Amazon deforestation, *J. Geophys. Res.* 107:8087. DOI:10.1029/2001JD000717.

Willmott, C. J.; Matsuura, K. 2001. Terrestrial air temperature and precipitation: Monthly and annual time séries (1950-1999). *Center for Climate Research*. version 1.02.

Woodward, M. R. L.; Kelly, C. K. 2004. Global climate and the distribution of plant biomes. *Philos Trans Roy Soc London.* 359B:1465–1476.

Yoon, J-H.; Zeng, N. 2010. An Atlantic influence on Amazon rainfall. *Clim. Dyn.* 34:249–264. DOI:10.1007/s00382-009-0551-6.

Xie, P.; Arkin, P. A. 1997. Global precipitation: A 17-year monthly analysis based on gauge observations, satellite estimates, and numerical model outputs. *Bull. Am. Meteorol. Soc*. 78:2539–2558.

Xu, L.; Samanta, A.; Costa, M. H.; Ganguly, S.; Nemani, R. R.; Myneni, R. B. 2011. Widespread decline in greenness of Amazonian vegetation due to the 2010 drought. *Geophys. Res. Lett.* 38:L07402. DOI:10.1029/2011GL046824.

APÊNDICE A – Descrição do Modelo IBIS

O modelo IBIS foi desenvolvido para conectar explicitamente processos de superfície terrestre e hidrológicos, ciclos biogeoquímicos terrestres e dinâmica da vegetação em uma única estrutura de modelagem (Foley et al., 1996; Kucharik et al., 2000). O modelo inclui representações de processos físicos da superfície (incluindo transferência de radiação solar e terrestre através do dossel, processos turbulentos, interceptação de água pelo dossel, transferência de massa e energia pelo dossel), fisiologia das plantas, fenologia do dossel, diferenças de tipos funcionais de plantas, alocação de carbono e biogeoquímica do solo. Todos os processos do IBIS são organizados em módulos de forma hierárquica e operam em diferentes intervalos de tempo, variando de minutos a anos, permitindo um acoplamento de processos ecológicos, biofísicos e fisiológicos que ocorrem em diferentes escalas de tempo.

O módulo de superfície terrestre do IBIS simula o balanço de energia, água, carbono e momentum entre o sistema solo-vegetação-atmosfera. O modelo representa duas camadas de vegetação (árvores e gramíneas), oito de solo e três de neve. Ele representa a temperatura da superfície do solo (ou neve) e a do dossel, além da temperatura e umidade do ar dentro do dossel. As mudanças na temperatura e umidade são funções do balanço radiativo da vegetação e do solo, e dos fluxos difusivos e turbulentos de calor sensível e de vapor d'água. Esse módulo usa um intervalo de integração de 60 minutos para capturar o ciclo diurno (Kucharik et al., 2000).

A radiação solar é simulada através da aproximação *two-stream*, com cálculos separados para radiação direta e difusa no visível (0,4 - 0,7 μm) e no infravermelho (0,7 - 4,0 μm). A radiação infravermelha é simulada como se a camada de vegetação fosse um plano semi-transparente com a emissividade dependente da densidade foliar (Foley et al., 1996; Kucharik et al., 2000).

Os fluxos turbulentos e a velocidade do vento dentro do dossel são modelados com o uso de um perfil logaritmo simples, tanto acima como entre as camadas do dossel, e um modelo difusivo simples de movimento do ar entre cada camada. Uma função linear empírica da velocidade do vento é usada para estimar a transferência turbulenta entre o solo (ou neve) e o dossel inferior (Kucharik et al., 2000).

A evapotranspiração total da superfície terrestre é a soma de três fluxos do vapor d'água: evaporação do solo, evaporação da água interceptada pelo dossel e a transpiração do dossel. As taxas de evapotranspiração dependem da condutância estomática e são calculadas para cada tipo de vegetação dentro do dossel. O modelo descreve a interceptação e a precipitação (chuva e neve) no dossel para considerar no cálculo da evapotranspiração (Kucharik et al., 2000).

O IBIS usa a formulação multi-camadas do solo para simular as variações diurnas e sazonais de calor e umidade nos primeiros 12m de solo. As espessuras dessas oito camadas são (numa ordem que vai da superfície do solo até maiores profundidades): 0,10, 0,15, 0,25, 0,50, 1,0, 2,0, 4,0 e 4,0m. Em cada intervalo de integração, cada camada é descrita em termos de temperatura do solo, conteúdo volumétrico de água e conteúdo de gelo. A equação de Richard é usada para calcular a taxa de mudança de umidade no solo. O fluxo vertical de água é modelado de acordo com a Lei de Darcy. O balanço hídrico do solo é controlado pelas taxas de infiltração, evaporação, transpiração e pela redistribuição de água no perfil. Todos esses processos são influenciados pela textura do solo e quantidade de matéria orgânica (Kucharik et al., 2000).

Os processos fisiológicos envolvidos na fotossíntese e na condutância estomática regulam diretamente as trocas de vapor d'água e CO_2 entre a vegetação e a atmosfera. O IBIS assume que a fotossíntese líquida dentro do dossel é proporcional à radiação fotossinteticamente ativa absorvida (APAR) dentro do mesmo (Kucharik et al., 2000). A taxa da fotossíntese de plantas C3, que inclui todas as árvores e muitas herbáceas, é representada seguindo as equações de Farquhar (Farquhar et al., 1980). A taxa de fotossíntese bruta por unidade de folha, A_g (mol CO_2 m^{-2} s^{-1}), é expressa como:

$$A_g \approx min(Je, Jc) \tag{1}$$

onde Je e Jc (mol CO_2 m^{-2} s^{-1}) são as taxas de fotossíntese limitadas pela luz e pela enzima Rubisco, respectivamente.

A taxa de fotossíntese limitada pela luz é dada por:

$$Je = \alpha_3 Q_p \left(\frac{C_i - \Gamma}{C_i + 2\Gamma}\right) \tag{2}$$

onde α_3 é a eficiência quântica para absorção de CO_2 em plantas C3 (mol CO_2 $Einstein^{-1}$), Q_p é a densidade do fluxo de radiação fotossinteticamente ativa (PAR) absorvida pela folha

(Einstein m^{-2} s^{-1}), C_i é a concentração de CO_2 nos espaços intercelulares das folhas (mol mol^{-1}) e Γ é o ponto de compensação para fotossíntese bruta (mol mol^{-1}).

A taxa de fotossíntese limitada pela enzima Rubisco é dada por:

$$Jc = \frac{V_m(C_i - \Gamma)}{C_i + K_C\left(1 + \frac{[O_2]}{K_O}\right)} \quad (3)$$

onde K_c e K_o (mol mol^{-1}) são os coeficiente de Michaelis-Menten para CO_2 e O_2, respectivamente, e V_m é a capacidade máxima da enzima Rubisco (mol CO_2 m^{-2} s^{-1}) calculado com a seguinte fórmula:

$$V_m = V_{max} * tempvm * stresstu \quad (4)$$

onde V_{max} é o valor nominal da capacidade máxima da enzima rubisco, *tempvm* é a função de estresse devido a temperatura e *stresstu* é a função de estresse devido a umidade em todas as camadas do solo.

A taxa da fotossíntese de plantas C4 é definida como:

$$A_g \approx \min(Ji, Je, Jc) \quad (5)$$

onde Ji, Je e Jc são as taxas de fotossíntese limitadas pela luz, pela enzima Rubisco e pelo CO_2, respectivamente.

$$Ji = \alpha_4 Q_p \quad (6)$$

$$Je = V_m \quad (7)$$

$$Jc = kC_i \quad (8)$$

onde α_4 é a eficiência quântica para absorção de CO_2 em plantas C4 (mol CO_2 $Einstein^{-1}$) e k = 18.000*V_m (mol m^{-2} s^{-1}).

A respiração da folha, R_{leaf} (mol CO_2 m^{-2} s^{-1}), é determinado por

$$R_{leaf} = \gamma V_m \quad (9)$$

onde γ é o coeficiente de respiração da folha (Kucharik et al., 2000).

A taxa de fotossíntese líquida é o balanço entre os processos de absorção (A_g) e de liberação (R_{leaf}) de CO_2:

$$An = A_g - R_{leaf} \quad (10)$$

A taxa de respiração de manutenção da biomassa dos galhos e troncos (R_{stem}), e das raízes (R_{root}) são dadas por

$$R_{stem} = \beta_{stem}\lambda_{sapwood}C_{stem,i}f(T_{stem}) \quad (11)$$

$$R_{root} = \beta_{root}C_{root,i}f(T_{soil}) \quad (12)$$

onde β é o coeficiente da respiração de manutenção, $\lambda_{sapwood}$ é a fração viva da biomassa, C_{stem} e C_{root} são o carbono contido na biomassa dos galhos (e troncos) e das raízes, respectivamente, e f(T) é a função de temperatura de Arrenhius, dada por:

$$f(T) = e^{E_0\left(\frac{1}{15-T_0}-\frac{1}{T-T_0}\right)} \quad (13)$$

onde T é a temperatura (ºC) (dos galhos e troncos ou do solo), E_o é um fator de sensibilidade da temperatura, e T_o é a temperatura de referência.

A condutância estomática é calculada pela fórmula

$$g_{s,h_2o} = \frac{mA_n}{C_s}h_s + b \quad (14)$$

onde $g_{s,h2o}$ é a condutância estomática do vapor d'água na folha (mol h_2o $m^{-2}s^{-1}$), C_s é a concentração de CO_2 na superfície da folha (mol mol^{-1}), h_s é a umidade relativa do ar na superfície foliar, m e b são o grau de inclinação e o intercepto da relação condutância-fotossíntese.

Muitas plantas possuem um ciclo anual de aparecimento de folhas (árvores decíduas, gramíneas) e da atividade fisiológica (árvores tropicais). Esse ciclo está relacionado a eventos climáticos. O IBIS usa parametrizações de fenologia baseados em algoritmos desenvolvidos por Botta et al. (2000) que foram calibrados com medições de sensoriamento remoto.

O florescimento de plantas decíduas devido à temperatura ocorre quando os graus dia acumulados atingem um certo valor (150 graus dia para gramíneas e 100 graus dia para árvores). A queda das folhas das árvores ocorre quando: a temperatura média de 10 dias seguidos é menor que 0º C ou a temperatura do ar está 5º C acima da menor temperatura média mensal. A queda das folhas das gramíneas ocorre quando a temperatura média de 10 dias seguidos é menor que 0º C.

As plantas decíduas devido à seca (árvores tropicais decíduas, gramíneas) respondem a mudanças no balanço de carbono do dossel. O modelo calcula a média (10 dias seguidos) da

taxa de fotossíntese líquida, se essa média for negativa (respiração foliar excedeu a fotossíntese bruta), o modelo faz as folhas caírem (Kucharik et al., 2000).

O IBIS representa a cobertura vegetal com um conjunto de tipos funcionais de plantas (PFTs), cada PFT é caracterizado em função da biomassa (carbono nas folhas, galhos e troncos, e raízes) e do índice de área foliar (LAI). A definição de PFT é usada para diferenciar várias características importantes, incluindo a fisionomia básica (árvores, arbustos ou gramíneas), comportamento foliar (decídua ou não-decídua), formato da folha (largas ou pontudas) e fisiologia (plantas C3 ou C4). A distribuição geográfica de cada PFT é determinada de acordo com o clima, considerando a tolerância a baixas temperaturas e os requisitos de graus dia (Foley et al., 1996).

São considerados 12 PFTs no IBIS: floresta tropical, floresta tropical decídua devido à seca, floresta temperada, conífera temperada, floresta temperada decídua devido à temperatura, conífera boreal, floresta boreal decídua devido à temperatura, conífera boreal decídua devido à temperatura, arbustos, arbustos decíduos devido à temperatura, gramíneas de clima frio e gramíneas tropicais.

Em cada célula do modelo, podem existir vários PFTs simultaneamente. A competição entre PFTs é caracterizada pela habilidade das plantas de capturar recursos, em particular, a competição por luz e pela água. No futuro pode ser adaptada a competição por nutrientes. Os PFTs do dossel superior capturam a luz primeiro e sombreiam o dossel inferior. Entretanto, o dossel inferior captura a umidade do solo primeiro. Assim o modelo pode simular a competição entre árvores e gramíneas (Foley et al., 1996).

A competição entre PFTs numa mesma camada do dossel (entre biomas) se dá pela diferença do balanço anual de carbono resultante de estratégias ecológicas distintas, como diferenças na fenologia, no formato da folha e na fisiologia (Kucharik et al., 2000).

O balanço anual de carbono para cada PFT é calculado somando os fluxos horários de carbono (fotossíntese bruta e os termos de respiração de manutenção). A produção primária bruta (GPP) de cada PFT i é calculada no final de cada ano como:

$$GPP_i = \int A_{g,i} dt \tag{15}$$

onde a integração é feita para o ano inteiro.

A produção primária líquida (NPP) de cada PFT é determinada por:

$$NPP_i = (1 - \eta) \int \left(A_{g,i} - R_{leaf,i} - R_{stem,i} - R_{root,i}\right) dt \tag{16}$$

onde η é a fração de carbono perdido devido a respiração de crescimento (Kucharik et al., 2000).

Cada PFT é representado em função de três divisões da biomassa: nas folhas, galhos e troncos, e raízes. O carbono nas folhas também pode ser expresso em termos do LAI multiplicado pela área foliar específica. As mudanças em cada compartimento j (folhas, galhos e troncos, e raízes) da biomassa de cada PFT i são descritas pela equação diferencial:

$$\frac{\partial C_{i,j}}{\partial t} = a_{i,j} NPP_i - \frac{C_{i,j}}{\tau_{i,j}} \quad (17)$$

onde $a_{i,j}$ representa a fração do NPP anual alocado para cada compartimento da biomassa e $\tau_{i,j}$ é o tempo médio de residência (representa as perdas por mortalidade, distúrbios e substituição de tecidos) de cada compartimento da biomassa.

O LAI é a razão entre a área da superfície de folha superior total da vegetação e área da superfície do solo na qual a vegetação cresce. No IBIS, o LAI é calculado pela soma dos LAIs da cada PFT representado pelo modelo:

$$LAI = \sum_{j=1}^{N} cbiol_j * specla_j \quad (18)$$

onde N é o numero de PFT representados no modelo, *specla* é área de folha específica e *cbiol* é o carbono no reservatório de biomassa de folha, calculado pela fórmula:

$$cbiol = cbiol * e^{\left(-\frac{1}{tau_{leaf}}\right)} + a_{leaf} * tau_{leaf} * max(0, aynpp) * \left[1 - e^{\left(-\frac{1}{tau_{leaf}}\right)}\right] \quad (19)$$

onde tau_{leaf} é o tempo de retorno do carbono nas folhas, a_{leaf} é a fração de alocação de carbono para as folhas e aynpp é a NPP total anual.

As mudanças do C nos reservatórios de biomassa são dadas pelas seguintes fórmulas:

$$outcrs = \min(decomps * krs * clitrs, clitrs) \quad (20)$$

$$outcws = \min(decompl * kws * clitws, clitws) \quad (21)$$

$$outcls = \min(decompl * kls * clitls, clitls) \quad (22)$$

$$outcnb = \min(decomps * knb * csoislon, csoislon) \quad (23)$$

$$outcpb = \min(decomps * kpb * csoislop, csoislop) \quad (24)$$

onde *outcrs*, *outcws* e *outcls* são as quantidades de C saindo dos reservatórios de carbono estrutural de raízes, madeira e folhas, respectivamente. *outcnb* é o fluxo de matéria orgânica não protegida para a biomassa e *outcpb* é o fluxo de matéria orgânica protegida para a biomassa. *krs*, *kws* e *kls* são as constantes de decomposição para os reservatórios de liteira estrutural de raízes, madeira e folhas, respectivamente. *kpb* e *knb* são as mesmas constantes, porém para a matéria orgânica protegida e não protegida, respectivamente. *decomps* é um fator de decomposição de matéria orgânica do solo e *decompl* é um fator de decomposição de liteira.

A equação básica de alocação de carbono é:

$$\frac{dC_r}{dt} = a_r NPP_{(t)} - \frac{C_r}{\tau_r} - \delta C_r \quad (25)$$

onde C_r é o estoque de carbono, a_r é o coeficiente de alocação, τ_r é o tempo de e δ é a taxa de distúrbios (incêndios, insetos, pastoreio, etc.).

No IBIS, o carbono fixado pela fotossíntese pode ser alocado em três diferentes compartimentos das plantas: folhas (a_{leaf}, τ_{leaf}), galhos e troncos (a_{stem}, τ_{stem}) e raízes (a_{root}, τ_{root}). Tanto os tempos de residência como os coeficientes de alocação são fixos. O somatório $a_{leaf} + a_{stem} + a_{root}$ é igual a 1. Esses coeficientes possuem incertezas e é comum o ajuste deles para a calibração do modelo, mas a soma dos coeficientes de alocação deverá ser sempre 1. Devido a dificuldades de parametrização da taxa de distúrbios, ela não é considerada como padrão no IBIS. A Tabela 1 mostra os coeficientes de alocação e os tempos de residência definidos no IBIS como o padrão para cada PFT.

O IBIS representa a distribuição vertical do sistema radicular de acordo com a equação proposta por Jackson et al. (1997):

$$y(d) = \frac{1-\beta_2^d}{1-\beta_2^{dmax}} \quad (25)$$

onde *Y (d)* é a fração de raízes finas entre a superfície e a profundidade do solo *d*, *dmax* é a profundidade máxima do solo e β_2 é um parâmetro de distribuição de raízes finas.

O IBIS permite o aumento da biomassa microbiana como uma função direta da quantidade de substrato disponível. O crescimento microbiano e a taxa de mineralização do nitrogênio são dependentes da textura do solo. O carbono da biomassa microbiana é mantido separado do carbono oriundo do solo. A atividade microbiana é dependente da função Arrenhius e da água contida nos poros. São usados perfis de raízes, que permitem que os

valores de umidade e temperatura do solo sejam ponderados de acordo com a localização aproximada da maioria da biomassa de carbono e microbiana (Kucharik et al., 2000).

O código do IBIS é disponibilizado gratuitamente e está escrito em Fortran 77.

Tabela 1 – Coeficiente de alocação e tempos de residência utilizados no IBIS para cada compartimento de cada PFT.

PFT	a_{leaf}	a_{root}	a_{stem}	τ_{leaf} anos	τ_{root} anos	τ_{stem} anos
Floresta tropical	0,30	0,20	0,50	1,00	1,0	25
Floresta tropical decídua	0,30	0,20	0,50	1,00	1,0	25
Floresta temperada	0,30	0,20	0,50	1,00	1,0	25
Conífera temperada	0,30	0,40	0,30	2,00	1,0	50
Floresta temperada decídua	0,30	0,20	0,50	1,00	1,0	50
Conífera boreal	0,30	0,40	0,30	2,50	1,0	100
Floresta boreal decídua	0,30	0,20	0,50	1,00	1,0	100
Conífera boreal	0,30	0,20	0,50	1,00	1,0	100
Arbustos	0,45	0,40	0,15	1,50	1,0	5
Arbustos decíduos	0,45	0,35	0,20	1,00	1,0	5
Gramíneas de clima frio	0,45	0,55	0,00	1,50	1,0	-
Gramíneas tropicais	0,45	0,55	0,00	1,25	1,0	-

Fonte: Kucharik et al., 2000.